





## Article

# Esterification of Kenaf Core Fiber as a Potential Adsorbent for Oil Removal from Palm Oil Mill Effluent (POME)

Nor Halaliza Alias <sup>1,2,\*</sup>, Luqman Chuah Abdullah <sup>1,\*</sup>, Thomas Choong Shean Yaw <sup>1</sup>, Siti Nurul Ain Md Jamil <sup>3</sup>, Teo Ming Ting <sup>4</sup>, Ahmad Jaril Asis <sup>5</sup>, Chuan Li Lee <sup>6</sup> and Abel Adekanmi Adeyi <sup>7</sup>

<sup>1</sup> Department of Chemical and Environmental Engineering, Faculty of Engineering, Universiti Putra Malaysia, Serdang 43400, Selangor, Malaysia; csthomas@upm.edu.my

<sup>2</sup> School of Chemical Engineering, College of Engineering, Universiti Teknologi MARA, Shah Alam 40450, Selangor, Malaysia

<sup>3</sup> Department of Chemistry, Faculty of Science, Universiti Putra Malaysia, Serdang 43400, Selangor, Malaysia; ctnurulain@upm.edu.my

<sup>4</sup> Radiation Processing Technology Division, Malaysian Nuclear Agency, Kajang 43000, Selangor, Malaysia; tmting@nm.gov.my

<sup>5</sup> Sime Darby Research Sdn. Bhd., Lot 42700, Pulau Carey, Banting 42960, Selangor, Malaysia

<sup>6</sup> Faculty of Biotechnology and Biomolecular Sciences, Universiti Putra Malaysia, Serdang 43400, Selangor, Malaysia; chuanli@upm.edu.my

<sup>7</sup> Department of Chemical and Petroleum Engineering, College of Engineering, Afe Babalola University Ado-Ekiti (ABUAD), PMB 5454, Ado-Ekiti 360211, Ekiti State, Nigeria; abeladeyi@abuad.edu.ng

\* Correspondence: norhalaliza@uitm.edu.my (N.H.A.); chuah@upm.edu.my (L.C.A.)

**Abstract:** Palm oil mill effluent (POME) is a major contributor to industrial oily wastewater in Malaysia, demanding effective treatment solutions. This study explores the potential of esterified kenaf core (EKC) fiber as an oil adsorbent for oil removal from POME, optimized using a full central composite design (CCD) within the response surface methodology (RSM) framework. The optimum conditions achieved 76% oil removal efficiency, with a 1:0.5 ratio of mercerized kenaf core to stearic acid (MKC:SA), 15 wt% of catalyst, and 1 h reflux time during the esterification process. The regression model exhibited strong predictive capability, with a significant quadratic correlation and an  $R^2$  value of 0.94. The Fourier transform infrared (FTIR) spectroscopy revealed the existence of ester functional groups characterized by significant hydrophobicity and a decrease in hydroxyl groups, indicating the chemical changes of EKC. Moreover, the scanning electron microscopy (SEM) research demonstrated structural alterations in EKC, including heightened surface roughness, fibrillation, and pore development, which improved oil adhesion relative to raw kenaf core (RKC). These findings indicate that EKC provides an effective, environmentally sustainable solution for managing oil wastewater issues in the palm oil sector, facilitating enhanced ecological sustainability and resource management.

**Keywords:** palm oil mill effluent (POME); oily wastewater; oil removal; adsorption; kenaf core; esterification



Academic Editor: Iqbal M. Mujtaba

Received: 30 December 2024

Revised: 25 January 2025

Accepted: 4 February 2025

Published: 8 February 2025

**Citation:** Alias, N.H.; Abdullah, L.C.; Yaw, T.C.S.; Jamil, S.N.A.M.; Ting, T.M.; Asis, A.J.; Lee, C.L.; Adeyi, A.A. Esterification of Kenaf Core Fiber as a Potential Adsorbent for Oil Removal from Palm Oil Mill Effluent (POME).

*Processes* **2025**, *13*, 463. <https://doi.org/10.3390/pr13020463>

**Copyright:** © 2025 by the authors.

Licensee MDPI, Basel, Switzerland.

This article is an open access article distributed under the terms and conditions of the Creative Commons Attribution (CC BY) license

(<https://creativecommons.org/licenses/by/4.0/>).

## 1. Introduction

The management of oily wastewater has emerged as a crucial area of investigation owing to its intricate composition and considerable environmental consequences. This wastewater, typically generated by industrial processes, encompasses a variety of pollutants, including oils and grease [1], petroleum derivatives such as gasoline, kerosene, and diesel [2], and elevated levels of dissolved organic and inorganic compounds [1,3]. Its dangerous characteristics present a significant risk to ecosystems, human health, and

natural resources. In 2020, the global discharge of oily wastewater worldwide has been expected to reach 54 billion m<sup>3</sup> [4]. These contaminants are recognized for their capacity to disturb aquatic ecosystems, taint potable and groundwater supplies, diminish agricultural yields, impede animal development, and degrade environmental quality [1,5–9]. The dire effects highlight the necessity for creative and effective treatment techniques.

In Malaysia, palm oil mill effluent (POME) is a leading source of industrial oily wastewater. POME is a colloidal suspension consisting of 95–96% water, 0.6–0.7% oil and grease, and 4–5% total solids [6,7]. It has high biological oxygen demand (BOD) and chemical oxygen demand (COD) with the value of 50,000 mg/L and 25,000 mg/L, respectively, coupled with significant oil and grease content (4000–8000 mg/L), acidic pH (4–5), and discharged temperature of 80 to 90 °C. The Malaysian Department of Environment (DOE) mandates a maximum allowable limit of 50 mg/L for oil and grease in discharged POME. Meeting these standards requires advanced and effective treatment solutions to address the environmental challenges posed by POME [9–13].

Various treatment methods have been explored for POME, including anaerobic digestion (ponding system) [14], anaerobic sludge fixed film reactor [15], integrated anaerobic-aerobic bioreactor [16], anaerobic sludge blanket reactor [17], and co-digestion in a solar-assisted bioreactor [18]. Conventional treatments such as the ponding system have low operating costs and are more convenient. However, these anaerobic digestion treatments require a long retention time and a large area to treat the POME and produce an unpleasant odor [19,20]. The long treatment period is mostly due to the slow microbe growing rates [21]. Other existing treatments for POME have been addressed by [22,23], which include micro and ultrafiltration, coagulation, flotation, membrane reactor, electrocoagulation, and Fenton technology. These technologies tend to be inefficient, costly, time-consuming, operationally complex, or require highly skilled operators [24]. The oil residual from POME can also be removed using the solvent extraction method [25], sedimentation–flocculation–coagulation methods [26], or physiochemical treatment [27].

However, as emphasized by [28], coagulation alone is often ineffective for the complete removal of pollutants, leaving residual impurities in the effluent. Moreover, the presence of organic compounds in natural coagulants that do not participate in the coagulation process can result in dissolved organic matter remaining in the treated water, which may promote bacterial regrowth and lead to the formation of harmful disinfection by-products. This highlights the limitations of coagulation as a standalone treatment and underscores the need for additional treatment stages [29]. In this context, the adsorption process stands out as one of the most efficient and extensively used methods of wastewater treatment, efficiently targeting both organic and inorganic contaminants [7,9], and is particularly good at recovering residual oil in water [30]. This is due to its simplicity, cost-effectiveness, and minimal environmental impact. Unlike other methods, adsorption systems produce minimum sludge and allow for the regeneration and reuse of adsorbents [23,31,32]. However, the selection of a suitable adsorbent remains critical, as different sorbents might have distinct adsorption mechanisms and thus affect the efficiency of the adsorption in treating oily wastewater [7].

Natural sorbents, such as chitosan flakes and powder [9], rubber powder [13], sago bark [33], chitosan in empty fruit bunch (EFB) filter [34], natural zeolites [35], and raw kenaf core fiber [24], have been investigated for their ability to remove the oil from POME. While these materials are affordable and environmentally friendly, they often exhibit low hydrophobicity and low buoyancy, which limit their oil adsorption capacity [36,37]. To overcome these limitations, the surface of the natural sorbent was modified by changing the chemical structure, where the functional groups attached to natural fibers are changed to more hydrophobic groups to increase the oil adsorption capacity and its hydrophobicity

properties [36–41]. Recently, modified adsorbents were developed for the oil removal from POME. These include the modified empty fruit bunch (EFB) through acetylation [42], alginate and mangrove composite beads coated with chitosan (AMCBCC) [43], modified oil palm leave (OPL) and modified oil palm frond (OPF) using lauric acid [44], esterified sago bark (ESB) [33], and a magnetic composite prepared from palm shell-based carbon [45].

The utilization of fatty acid in increasing the hydrophobicity of the natural sorbent through an esterification reaction to produce an oil adsorbent has been reported. This includes modified plantain peel fiber (PPF) using stearic acid [46], esterified sago bark (ESB) using stearic acid [33], oleic and palmitic acid-treated bark (OTB and PTB) [41], modified banana trunk fibers using oleic acid [47], and sawdust grafted with oleic acid [48]. Fatty acid is used in esterification reactions to convert the hydroxyl group in the natural fiber into an ester group, which has high hydrophobic characteristics and hence increases the oil adsorption capacity [36].

Kenaf (*Hibiscus cannabinus* L.), a fast-growing fiber plant, is recognized as a sustainable resource due to its adaptability to various climates, rapid growth, and minimal crop rotation needs. It thrives under different environmental and soil conditions, making it suitable for industrial applications. The core fiber of kenaf, which makes up about 65% of its stem, has shown significant potential as a cost-effective adsorbent for wastewater treatment [49–51]. With a price of approximately RM500 per tonne, kenaf offers a cost-effective, environmentally friendly alternative that is widely available worldwide [52]. According to [53], the ground kenaf core is able to remove the oil from water, with an adsorption capacity of 3.95 g oil/g. To date, the use of kenaf has been extensively reported for several applications, such as paper, pulp and other fiber products, jeans, indoor panels and other interior components for high-end cars (BMW and Mercedes Benz), composite materials for buildings or the construction industry, brighter bulletproof vest, erosion control in the geotextiles industry and soil remediation for hydrocarbonate infestations [50], human and animal feed [54], filler or a natural anti-degradant in producing thermoplastic elastomer [55], and adsorption [56,57].

Notwithstanding its numerous applications, the utilization of kenaf as an oil adsorbent for the treatment of oily wastewater remains predominantly unexamined. In contrast to non-renewable resources like coal, which is frequently utilized in energy generation and industrial applications, and valued at roughly \$115 per ton in January 2025 [58], kenaf offers a cost-effective and renewable alternative for wastewater treatment. Its cost-effectiveness, coupled with its worldwide accessibility, renders it a suitable option for sustainable industrial practices. Chemical modifications to kenaf may enhance its properties, rendering it an effective and environmentally sustainable adsorbent. Creating kenaf-derived adsorbents for industrial wastewater treatment can diminish dependence on limited resources such as coal, lessen environmental repercussions, and promote sustainable industrial methodologies.

This study focuses on the modification of raw kenaf core (RKC) fiber through mercerization and esterification with stearic acid to produce esterified kenaf core (EKC) fiber as an efficient oil adsorbent for POME treatment. This reaction replaces the hydroxyl groups in MKC with ester groups, which exhibit strong hydrophobic characteristics. The hydroxyl group, being a reactive functional group, is highly susceptible to chemical modification. Stearic acid, a long-chain fatty acid with 18 carbon atoms, was selected due to its significant hydrophobicity and lipophilic properties [59], both of which are critical in improving the oil adsorption efficiency of EKC. Optimization of the production process was conducted using response surface methodology (RSM) with a central composite design (CCD), examining parameters such as the ratio of MKC to SA, the percentage of the catalyst (calcium oxide, CaO), and reflux time. The modified EKC is expected to exhibit superior hydrophobicity and oil adsorption capacity, offering a cost-effective and environmentally sustainable

solution for POME treatment. By advancing the development of natural adsorbents, this study addresses the pressing need for innovative and efficient wastewater management technologies in the palm oil industry.

## 2. Materials and Methods

### 2.1. Physical Treatment of POME

The palm oil mill effluent (POME) was collected from the sludge pit area at the Sime Darby KKS Labu Mill, Negeri Sembilan, Malaysia, at a temperature of 90 °C. The raw effluent (POME) was filtered using a muslin cloth strainer to remove millimeter-sized solid particles. The filtered POME was subsequently analyzed for pH, total solid, and oil and grease content. To preserve its properties, the sample was stored at 4 °C prior to the pretreatment.

### 2.2. Adsorbent Preparation

#### 2.2.1. Raw Kenaf Core Fiber Preparation

The kenaf stalks used in the present study were obtained from Lembaga Kenaf dan Tembakau Negara (LKTN), Kelantan, Malaysia. Initially, the entire stalks of raw kenaf core were chipped using a chipper mill to reduce them to a smaller size. The chipped raw kenaf core (RKC) was then thoroughly dried in an industrial oven set to 60 °C for 7 days to ensure that all moisture was removed. Following this, the chipped RKC was ground, washed with distilled water, and dried in the oven at 60 °C for 24 h. The material was sieved to a particle size of 2 mm using a stainless steel sieve shaker and kept in a desiccator until further use.

#### 2.2.2. Mercerization of Raw Kenaf Core (RKC) Fiber Preparation

A total of 10 g of raw kenaf core (RKC) fiber was immersed in a 20 wt% sodium hydroxide (NaOH) solution, prepared by dissolving 50 g NaOH in 250 mL of distilled water, for a duration of 24 h. Following the soaking process, the mercerized kenaf core (MKC) fibers were thoroughly rinsed with distilled water to remove any residual alkali. The washed fibers were then dried in an oven at 60 °C for 24 h to achieve consistent dryness before being utilized in the subsequent esterification reaction.

### 2.3. Single Factor Experiment

A single-factor experiment was conducted to determine the optimal range of oil removal from palm oil mill effluent (POME) for subsequent optimization in the esterification reaction. The range selected was based on a previous study conducted by [33]. Three independent parameters were studied within their respective ranges: the ratio of MKC to stearic acid (1:0.5, 1:1, and 1:2), percentages of catalyst (5 wt%, 10 wt%, and 15 wt%), and reflux time (1, 4.5, and 8 h). Each parameter was maintained at a constant level, while the effect of one factor was investigated by varying its level individually. The impact of each factor on the percentage of oil removal from POME was analyzed accordingly.

### 2.4. Design of Experiment (DOE) and Statistical Analysis

The response surface methodology (RSM) was applied using a statistical design experiment based on the central composite design (CCD). The analysis of the experimental data was conducted using Design-Expert Version 7.0.0 software [60]. In accordance with the result from the preliminary single-factor experiment, the independent variables with their corresponding levels were then applied to the CCD, with an alpha ( $\alpha$ ) value of  $\pm 1$ . The independent variables involved in EKC optimization were the MKC:SA ratio (factor A), percentages of catalyst (factor B), and refluxing time (factor C). The response in this study was the oil removal efficiency of EKC from POME. Each factor was studied at two levels,

which were the low level (−1) and the high level (+1). The central values (zero level) chosen for the experimental design were 1:1 (factor A), 10% (factor B), and 4.5 h (factor C). Table 1 shows the analyzed factors and their respective notations and levels. The value ranges of MKC:SA, catalyst percentage, and refluxing time were chosen based on single-factor experiments.

**Table 1.** Parameters of oil removal efficiency of EKC from POME and the respective treatment levels.

Notation	Factor	Unit	Actual Value		
			Low Level (−1)	High Level (+1)	Mean (0)
A	MKC:SA ratio	-	0.5	1.5	1.0
B	Percentage of catalyst	%	5	15	10
C	Refluxing time	hours	1	8	4.5

The experimental response, which refers to the percentage of oil removal from POME attained at distinct combinations of the factors' levels, was then used to initiate an empirical regression model relating to the studied factors based on the second-order polynomial model as shown in Equation (1):

$$y = \beta_0 \sum_{i=1}^k \beta_i x_i + \sum_{i=1}^k \beta_{ii} x_i^2 + \sum_{i=1}^k \sum_{j=i+1}^{k-1} \beta_{ij} x_i x_j \quad (1)$$

where  $y$  is the response variable, which is the oil removal from POME (%);  $\beta_0$ ,  $\beta_i$ ,  $\beta_{ii}$ , and  $\beta_{ij}$  are the regression coefficients for the intercept, linear, quadratic, and interaction, respectively;  $x_i$  and  $x_j$  are the independent variables (factors) influencing the response values; and  $k$  is the number of studied variables. The analysis of variance (ANOVA) provided a statistical analysis, where it revealed the correlation between all the factors involved, the significant of each factor tested, and the accuracy of the developed model. Meanwhile, the adequacy of the fitted model was assessed through the residual analysis. All statistical evaluations considered a 5% significance level, where the  $p$ -values were required to be less than 0.05.

### 2.5. Esterification Reaction

The mercerized kenaf core (MKC) (4 g) was placed in a 500 mL three-neck round-bottom flask containing 100 mL of ethyl acetate as the reaction medium. Stearic acid was introduced according to the specified MKC-to-stearic acid ratios of 1:0.5, 1:1, and 1:1.5. Calcium oxide (CaO) was used as the catalyst and added at 5 wt%, 10 wt%, and 15 wt%, respectively, relative to the mass of MKC. The esterification reaction was conducted under reflux conditions for durations of 1 h, 4.5 h, and 8 h, depending on the experimental design. Upon completion of the reaction, the mixture was filtered to separate the modified fibers. The product was subsequently washed with ethanol and then acetone to remove unreacted materials and impurities. The esterified kenaf core (EKC) was dried in an oven at 40 °C for 3 h. After drying, the EKC was cooled to ambient temperature and stored in a desiccator to prevent moisture absorption prior to further analysis. The esterification apparatus utilized in this study is depicted in Figure 1.



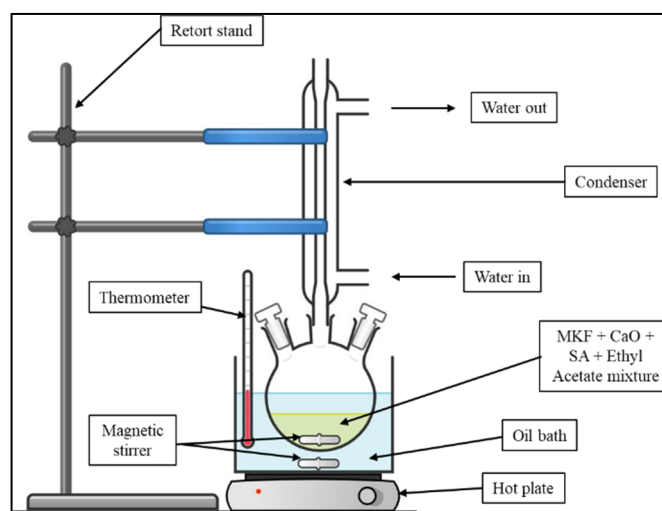


**Figure 1.** Setup of the esterification reaction.

## 2.6. Application of Esterified Kenaf Core on POME

The oil removal efficiency of the esterified kenaf core (EKC) was evaluated using palm oil mill effluent (POME). A sample of 0.08 g of EKC was mixed with 20 mL of POME and stirred at 130 rpm for 30 min at ambient temperature using a magnetic stirrer. Following the reaction, the mixture was filtered, and the filtrate was collected for oil and grease analysis. All experiments were performed in triplicate to ensure the reliability and consistency of the results.

## 2.7. Determination of Oil and Grease (O&G) Content in POME

The oil content in POME was determined using a hexane extraction method, adhering to the guidelines outlined in the Standard Methods for the Examination of Water and Wastewater, Section 5520B [61]. Approximately 20 mL of the filtrate (treated POME) was transferred into a separatory funnel. A 1:1 hydrochloric acid (HCl) to water solution was prepared, and 0.5 mL of this solution was added to the filtrate to adjust the pH  $\leq 2$  before introducing 3 mL of hexane. The mixture was vigorously shaken for 2 min and allowed to settle for 10 min to form two distinct layers.

The organic and oil-containing layer was separated by gravity filtration, with the procedure repeated in triplicate for accuracy. The collected filtrate was dried over 2 g of anhydrous sodium sulfate ( $\text{Na}_2\text{SO}_4$ ). After drying, the  $\text{Na}_2\text{SO}_4$  was separated from the oil using Whatman No. 40 filter paper. Residual hexane in the oil sample was removed using a rotary evaporator (Heidolph Laborota 4000 Efficient) operated for 15 min to ensure complete solvent removal. The oil sample was subsequently dried in an oven at 103 °C for 10 min, cooled to room temperature, and weighed. The weight of the oil sample was recorded as the oil and grease (O&G) content, which was calculated using Equation (2):

$$\text{O\&G} \left( \frac{\text{mg}}{\text{L}} \right) = \left[ \left( \frac{(W_f - W_i) \text{g} \times 1000 \frac{\text{mg}}{\text{g}}}{V(\text{L})} \right) \right] \quad (2)$$

where  $W_f$  and  $W_i$  are the final and initial weight of the flask, respectively (g); and  $V$  is the volume of POME (L).

Meanwhile, the oil removal efficiency can be determined from Equation (3):

$$\text{Oil removal efficiency}(\%) = \left[ \frac{C_o - C}{C_o} \right] \times 100\% \quad (3)$$

where  $C_0$  and  $C$  are the initial oil and grease concentration (mg/L) in POME and the oil and grease concentration (mg/L) in the filtrate, respectively [33,45].

## 2.8. Preliminary Adsorption Analysis

The adsorption capacity of RKC and EKC for oil removal from POME was investigated at varied initial pH values (2–8) as a typical case study. The batch experiment was performed using 0.4 g of RKC and EKC, respectively, which were mixed with 100 mL of POME. The mixture was stirred under constant speed at 200 rpm at 30 °C (room temperature) for a contact time of 30 min. The oil removal from POME was analyzed according to the procedure described in Section 2.7. The experiments were performed in triplicate, and the average values were recorded.

## 2.9. Characterization

### 2.9.1. Attenuated Total Reflectance—Fourier Transform Infrared Spectroscopy (ATR-FTIR)

ATR-FTIR analysis was performed using a Perkin-Elmer Spectrum 100 model (Perkin-Elmer (M) Sdn. Bhd., Petaling Jaya, Malaysia). The technique employs infrared light to scan samples and detect characteristic chemical bonds and functional groups [62]. Both raw kenaf core (RKC) and esterified kenaf core (EKC) fibers were analyzed to assess whether the intended modifications were successfully achieved, particularly by observing changes in their functional groups.

### 2.9.2. Scanning Electron Microscopy (SEM)

In this study, the surface morphology of raw kenaf core (RKC) and esterified kenaf core (EKC) fiber was observed using an S-3400N SEM (Hitachi, Hi-Tech Instrument Sdn. Bhd., Puchong, Malaysia) at magnifications of 100× and 600×, respectively [63].

## 3. Results and Discussions

### 3.1. Reaction Mechanism of Esterification Reaction

Figure 2 shows the reaction mechanism between the hydroxyl group from RKC, CaO, and SA in the esterification reaction. The purpose of using CaO was to deprotonate the abundant hydroxyl group in cellulose [33]. The alkoxide ion produced after deprotonation reacted with SA, which finally produced an ester group that has the ability to adsorb the oil from POME due to its high hydrophobicity compared to MKC and RKC.

### 3.2. Single Factor Experiment

The analysis of the individual effect of each independent factor associated with the oil removal efficiency was examined using a single-factor experiment. Furthermore, it provides a practical range for consecutive optimization studies. The range covered in this study included the ratio of MKC to SA (MKC:SA), the percentages of catalyst, and the reflux time of the esterification reaction.

#### 3.2.1. Effect of the Ratio of MKC to Stearic Acid (MKC:SA)

Figure 3a shows the effect of the ratio of MKC:SA ranging from 1:0.5, 1:1, and 1:2. The amount of catalyst percentage and reflux time were fixed at 5 wt% of MKC and 1 h, respectively. As the amount of SA increased, oil removal efficiency decreased noticeably. At a ratio of 1:0.5, the efficiency was measured at 75.3%, but at 1:2, it dropped to 42.4%. Due to an excess of SA in the reaction, the ratio should not be greater than 1:1. This is evidenced by the existence of a white solid SA residue that partially coated the surface of EKC following the 1:2 ratio experiment (Figure 4). Furthermore, the higher ratio (mass) of SA to MKC would increase the demand for ethanol to remove excess SA from the EKC

surface. This excessive use of ethanol renders the washing process economically inefficient, especially with the elevated amount of SA. Therefore, it can be concluded that the lowest amount of SA, with a ratio of 1:0.5 (MKC:SA), was adequate to esterify the MKC in this single-factor study, as it gave the highest oil removal efficiency (75.3%).

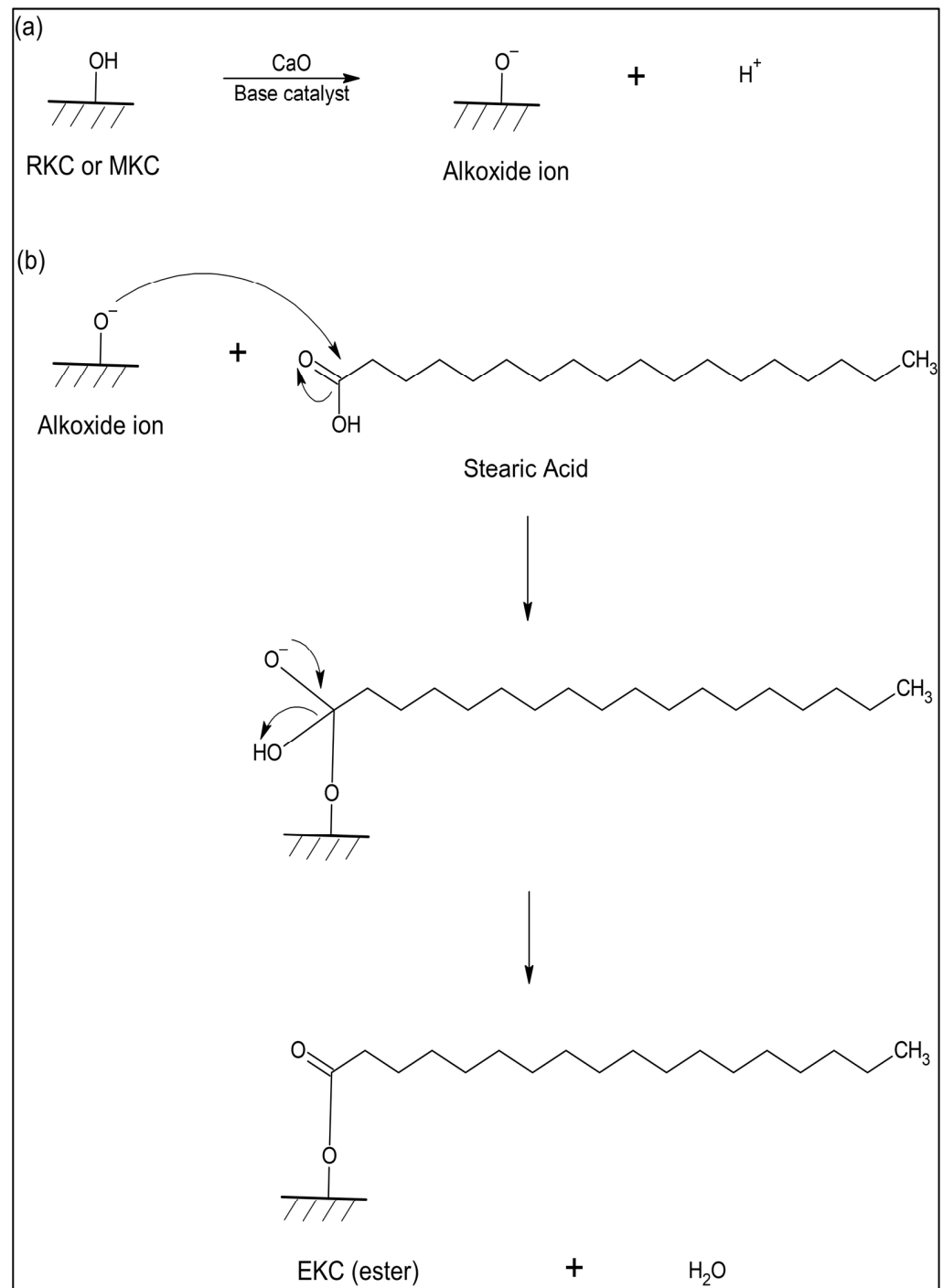


**Figure 2.** Proposed reaction mechanism of esterification starting from (a) the deprotonation of RKC or MKC, followed by (b) the esterification reaction with stearic acid to produce an ester (EKC).



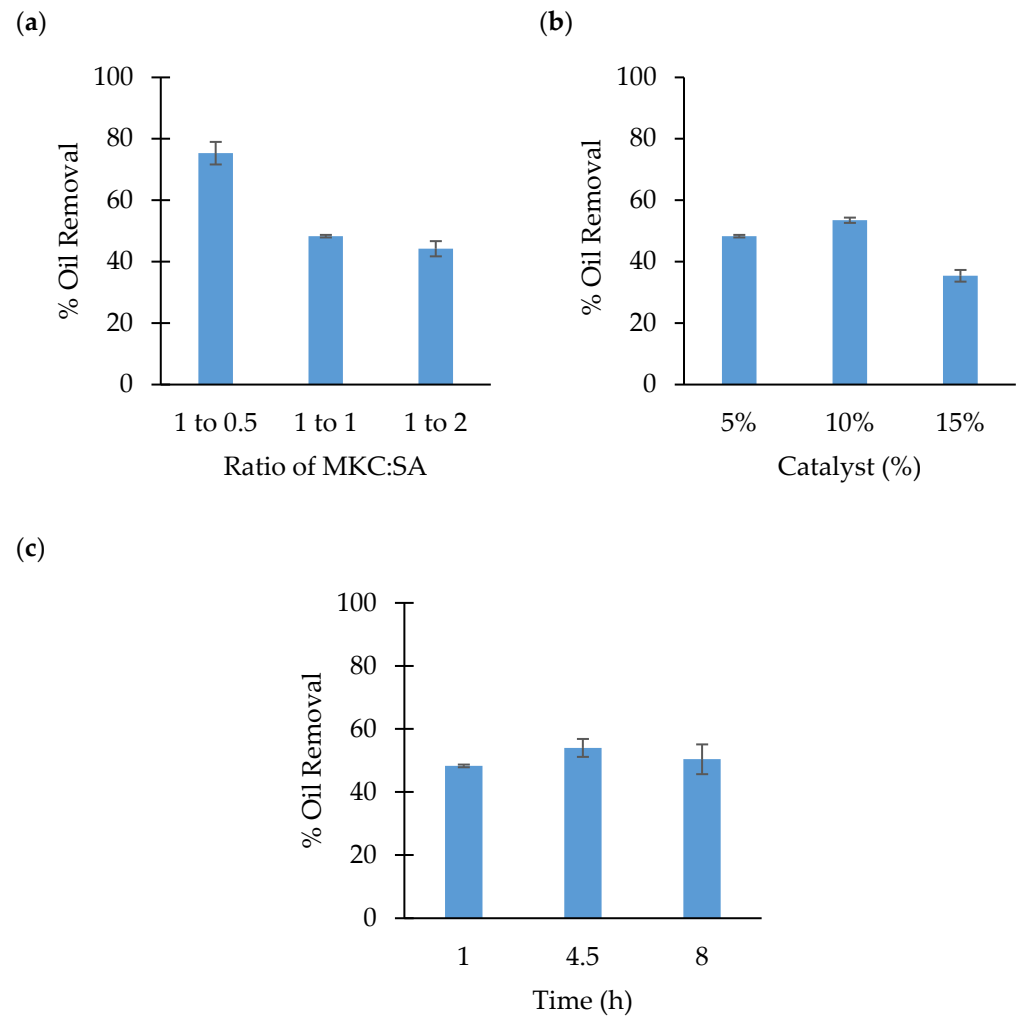


**Figure 3.** Single factor experiment for (a) the effect of the ratio of MKC:SA, (b) the effect of the catalyst, and (c) the effect of refluxing time on oil removal efficiency from POME through the esterification reaction.



**Figure 4.** White solid SA residue partially coating the surface of EKC at an MKC:SA ratio of 1:2 (reaction condition: 5 wt% of CaO and 1 h of reflux time).

### 3.2.2. Effect of Catalyst Percentages

The effect of catalyst percentages ranged from 5 wt%, 10 wt%, and 15 wt% of MKC. The ratio of MKC:SA was fixed at 1:1, with a reflux time of 1 h. Referring to Figure 3b, it is apparent that as the catalyst percentage increased from 5 wt% to 10 wt% of MKC, there was a corresponding rise in the oil removal efficiency. Oil removal efficiencies at these catalyst

percentages were 48.3% and 53.5%, respectively. This observation can be attributed to the higher catalyst percentage added into the reaction, which induces more hydroxyl groups in the MKC structure to deprotonate [64]. Consequently, this results in more SA attaching to the MKC surface, ultimately leading to an increase in the oil removal efficiency. However, the graph showed a significant decrease in oil removal efficiency from POME when using EKC, which fell to 35.4% as the percentage of catalyst increased to 15 wt% of MKC. This was probably because the addition of 15 wt% was not suitable, as this amount might be too immoderate for this experiment setup, which used a 1:1 ratio of MKC:SA and a 1 h reflux time. The addition of excess catalyst caused a saponification reaction to occur due to the existence of the calcium hydroxide ( $\text{Ca(OH)}_2$ ) compound in CaO, which has basic properties. Furthermore, the saponification reaction made the solution too viscous, making it difficult for CaO to dissolve when present in excess [65,66].

It was also noticeable that the solvent (ethyl acetate) used in this reaction became cloudy (Figure 5) when 15 wt% (CaO amount) was used compared to 5 wt% due to the excess CaO amount at a 1 h reflux time. The reaction between CaO and water (a byproduct of the esterification reaction) produced  $\text{Ca(OH)}_2$ , which caused the formation of a cloudy solvent [65,67]. Another possible reason for the cloudy solvent was the unstable nature of calcium oxide, which tends to leach into the reaction medium [68]. Figure 3b reveals that a 10 wt% catalyst amount achieved the highest oil removal efficiency from POME using EKC, reaching 53.5% in this single-factor study.

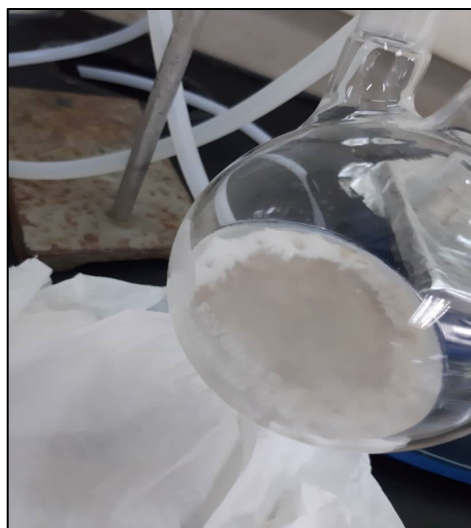


**Figure 5.** Appearance of cloudy solvent after using 15 wt% of catalyst (CaO) in the esterification reaction (reaction condition: MKC:SA ratio of 1:1 and 1 h of reflux time).

### 3.2.3. Effect of Refluxing Time

Figure 3c depicts the effect of reflux time in the esterification reaction. The range studied was between 1 h, 4.5 h, and 8 h. The time was set to be limited to 8 h of operation only to simulate the normal operation in the chemical industry [69]. In the effect of reflux time, the ratio of MKC:SA and percentage of catalyst were set at 1:1 and 5 wt% of MKC, respectively. The graph shows that the oil removal efficiency increased as the reflux time increased from 1 h (48.3%) to 4.5 h (54.0%), whereby a longer refluxing time exposed the MKC surface and ultimately increased the number of ester sites. Thus, high oil removal efficiency was achieved with a longer refluxing time. Nevertheless, Figure 3c shows the deterioration of oil removal efficiency from POME to 50.4% at 8 h (after long hours of operation). This was attributed to the formation of a white solid (residual SA, which appeared after 4.5 h of reflux time) on the EKC surface, where the layer is fully

coated with the white solid. The increase in reflux time beyond the optimum might cause the esterification reaction to proceed in the backward direction since the reaction is reversible [70]. This led to an increase in the acid value (SA) used in this experiment. Based on Figure 3c, the reflux time of 4.5 h yielded the maximum oil removal efficiency, at 54.0% in this single-factor study.

### 3.3. Optimization of Esterified Kenaf Core (EKC) Using RSM

#### 3.3.1. Fitting the Model and Analysis of Variance (ANOVA)

A central composite design (CCD) was performed by measuring the esterification factors, namely, the ratio of MKC:SA, the percentage of catalyst, and reflux time. A design matrix comprising 18 single-block experiments, conducted in a randomized order with six repetitions at the center point, was produced. The main objective of this research was to obtain optimized oil removal efficiency (Response). Therefore, the actual esterification factors and the average response are presented in Table 2.

**Table 2.** Design matrix based on CCD with experimental response data of oil removal efficiency from POME through the esterification reaction.

Run	Factor A	Factor B	Factor C	Average Response	Predicted Value	Residual Error (%)
	A: Ratio of MKC:SA	B: Percentage of Catalyst (%)	C: Refluxing Time (h)	Y: Oil Removal Efficiency (%)		
1	1	10	4.5	60.5	64.25	5.84
2	0.5	15	8	71.5	71.56	0.08
3	1.5	5	8	71.8	71.60	0.28
4	0.5	5	8	72.2	71.85	0.48
5	0.5	15	1	76.0	76.21	0.28
6	1	10	4.5	64.2	64.25	0.08
7	1	10	4.5	63.5	64.25	1.17
8	1	10	4.5	66.8	64.25	3.82
9	1.5	15	8	75.3	75.21	0.12
10	0.5	5	1	74.2	74.30	0.14
11	1	10	1	74.7	74.10	0.80
12	1.5	15	1	69.6	69.95	0.50
13	1	10	8	74.9	75.50	0.79
14	1	10	4.5	65.9	64.25	2.50
15	1	15	4.5	73.3	72.78	0.71
16	1	10	4.5	64.6	64.25	0.54
17	1	5	4.5	69.5	70.02	0.74
18	1.5	5	1	64.2	64.15	0.08

The data obtained from the experimental value (Response) were fitted to a second-order polynomial equation. The empirical quadratic model for the oil removal efficiency, Y (%), with coded factors, is shown in Equation (4):

$$Y(\%) = +64.25 - 1.63A + 1.38B + 0.70C + 0.98AB + 2.48AC - 0.55BC - 10.10A^2 + 7.15B^2 + 10.55C^2 \quad (4)$$

Equation (4) presents the regression model, which involves all terms, including the linear terms (A, B, C), the interaction terms (AB, AC, BC), the quadratic terms ( $A^2$ ,  $B^2$ ,  $C^2$ ), and their respective regression coefficient values. The positive and negative signs in the linear terms demonstrate increasing and decreasing factor levels, respectively [71]. Analysis of variance (ANOVA) serves to analyze the adequacy and quality of the fitted model. Additionally, ANOVA helps distinguish the variation of change in the combination

of factor levels (treatments) from the variation due to random errors, allowing for the measurement of the generated responses.

Table 3 shows the ANOVA summary for the esterification reaction, representing the significance of the model terms, including linear, interaction, and quadratic terms. According to [72], the analysis is also important to validate the accuracy, credibility of the model, and goodness-of-fit of the quadratic model (Equation (4)) obtained from the experimental results. The second-order polynomial model can be confirmed as either significant or not significant using ANOVA analysis.

**Table 3.** Analysis of variance (ANOVA) for the esterification reaction.

Source	Sum of Squares	Mean Square	F Value	p-Value (Prob > F)	
Model	376.89	41.88	13.09	0.0007 *	Significant
A-MKC:SA	21.13	21.13	6.6	0.0332 *	
B-% Catalyst	19.04	19.04	5.95	0.0406 *	
C-Time	4.9	4.9	1.53	0.251	
AB	7.61	7.61	2.38	0.1617	
AC	49.01	49.01	15.32	0.0045 *	
BC	2.42	2.42	0.76	0.4098	
A <sup>2</sup>	78.98	78.98	24.68	0.0011 *	
B <sup>2</sup>	76.68	76.68	23.97	0.0012 *	
C <sup>2</sup>	166.95	166.95	52.18	<0.0001 **	
Residual	25.6	3.2			Not Significant
Lack of Fit (LOF)	1.62	0.54	0.11	0.9489	
Pure Error	23.97	4.79			
Corrected Total	402.49				
Analysis of The Regression Equation					
Standard Deviation (SD)	1.79	R <sup>2</sup>	0.9364		
Mean	69.59	Adjusted R <sup>2</sup>	0.8649		
Correction of Variation (CV) in %	2.57	Predicted R <sup>2</sup>	0.8654		
PRESS	54.17	Adequate Precision	9.046		

\*  $p < 0.05$ , significant. \*\*  $p < 0.0001$ , highly significant.

Based on Table 3, the ANOVA results indicated that the quadratic model was statistically significant ( $p < 0.05$ ), suggesting that the model was the best fit for all experimental data collected on oil removal efficiency from POME using EKC. Among the model terms, the linear terms involving the ratio of MKC:SA (A) and the percentage of catalyst (B), the interaction terms of the ratio of MKC:SA and reflux time (AC), and the quadratic terms of the ratio of MKC:SA (A<sup>2</sup>), percentage of catalyst (B<sup>2</sup>), and reflux time (C<sup>2</sup>) were observed as statistically significant, with  $p$ -values less than 0.05. On the other hand, the remaining terms, namely the reflux time (C), interaction terms of the ratio of MKC:SA and the percentage of catalyst (AB), and the percentage of catalyst and reflux time (BC) were identified as insignificant since the  $p$ -values were greater than 0.05. According to Table 3, the most significant factor was the quadratic term of reflux time (C<sup>2</sup>), with the lowest  $p$ -value nearly approaching zero (<0.0001). This suggests that the quadratic factor of C<sup>2</sup> can highly influence oil removal efficiency. The strong nonlinearity (curvature) of reflux time (C) indicates a divergence in the oil removal response from POME as reflux time (C) increased. It shows that further increases in reflux time in the esterification may reduce oil removal efficiency from POME. This was due to the residual SA appearing in white solid

form on the EKC surface (fully coated) when the reflux time increased from 4.5 h to 8 h (as discussed in Section 3.2.3). Thus, more volume of ethanol is needed in the EKC washing process, which leads to an uneconomical effect. Improper washing of EKC can block its pores with SA and CaO, reducing its ability to adsorb oil from POME.

The fitness of the model was also evaluated through the lack of fit (LOF) analysis. A significant model should have a non-significant LOF, which proposes that the residual error (the difference between the observed response and the predicted response) has not exceeded the pure error produced from randomized replicated design points [73,74]. In this study, the  $p$ -value obtained for the LOF analysis was 0.9489 ( $p$ -value > 0.05), which indicated the insignificance of LOF. There was a 94.89% chance that a lack of fit F-value this large could occur due to noise. The F-value for LOF (0.11) also showed insignificance, comparable to the pure error of the experiment. Therefore, the second-order (quadratic model) suggested could be used to predict response values (oil removal efficiency).

The coefficient of determination ( $R^2$ ), also known as R-squared, is another critical measurement used to evaluate the fitness of the model. Basically, the R-squared value indicates how much of the data variation around the mean value (variance) of the observed responses can be accounted for by the model. Based on Table 3, it was observed that the R-squared value obtained in this study was 0.9364, suggesting that almost 93.64% of the variation in the oil removal efficiency response can be described by the independent variables, while only 6% of the variation cannot be described by the model [75]. Thus, the R-squared projected in this study showed the adequacy of the quadratic polynomial model, as a high R-squared value implies that the experimental values are well aligned with the predicted values.

The adequate precision measures the signal-to-noise ratio, where the range of the predicted values at the design point is compared to the average prediction variance. Based on this study, the adequate precision value obtained was 9.046. In order to have an adequate model, a ratio greater than 4 is desirable since this indicates the ability of the model to distinguish the origin of data variations. Thus, it signifies that the model can be used to navigate the design space. Besides, further verification of the model fitness could be done using the CV% (coefficient of variation) value. The CV% describes the degree of dispersion of the data points around the mean value. A lower value of CV% (preferably less than 10%) recommends a good reproducibility of the model [73]. The CV% value observed in this study was 2.57%, which indicates that the experimental value had high precision and excellent reliability [76,77] since it showed a low variation in the mean value [78].

The diagnostic plots of the predicted responses versus actual responses for oil removal efficiency from POME are presented in Figure 6a. Generally, a diagnostic plot provides a visual representation of data to evaluate the goodness-of-fit of model regression. The discrepancy between the predicted responses and actual responses can be envisaged through the fitted plots in Figure 6a. The data points were randomly dispersed along and close to the straight line, except for one point (blue) that deviated from the linear line with a residual of  $-3.75$  (5.84% error). However, the plots were consistent, signifying that the quadratic model was well fitted to obtain oil removal efficiency due to the high value of R-squared (0.9364).

Based on the normal probability plot in Figure 6b, the residuals were disseminated along the straight line, except for two points at the bottom left (blue and red) that deviated from the linear line with residuals of  $-3.75$  (5.84% error) and  $-0.6$  (0.79% error), respectively. Nevertheless, the normal probability plot of the residuals envisaged was approximately linear, supporting the condition that the error terms are normally distributed [79]. As reported by [74], residual data should be independent of each other and follow a normal distribution with constant variance. Thus, it was confirmed that the plot followed the

normal or linear distribution. Meanwhile, the plot of residual versus predicted responses portrays the suitability of the selected model and the correlation of the data. All the diagnostic plots (Figure 6a,b) confirmed that the ANOVA assumptions were satisfied based on the residual analysis above. Thus, the regression analysis produced the estimation of unbiased coefficient estimates with the least variance, suggesting the adequacy of the model in calculating oil removal efficiency.

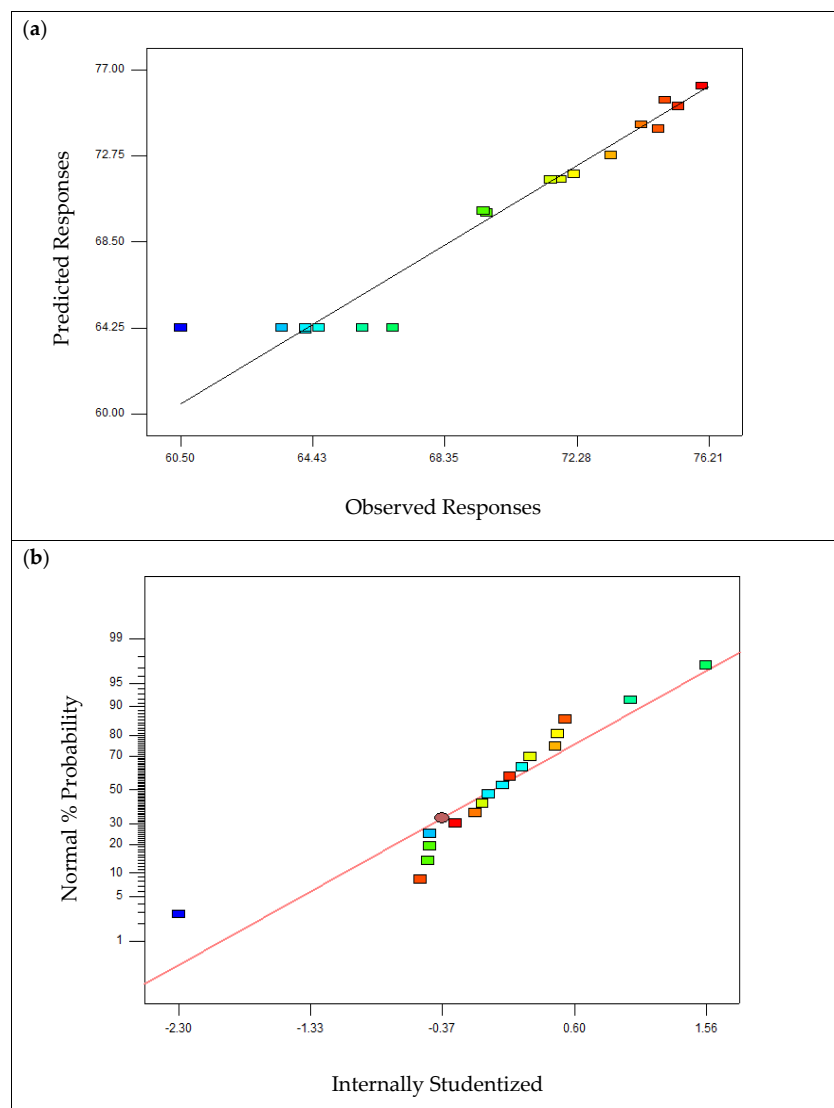


**Figure 6.** Diagnostic plots of (a) predicted responses vs. observed responses, and (b) the normal probability plot for the esterification reaction. The different color in the figure represents the data point plotted based on the Experiment Run. No.

### 3.3.2. Effect of Esterification Factors on Percentage Oil Removal from POME in Response Surface Plots Analysis

Figure 7a presents the surface and contour plots of oil removal efficiency as a function of the MKC:SA ratio (A) and catalyst percentage (B) at a constant reflux time (C) of 4.5 h. The maximum oil removal efficiency of EKC was 73.3%, which corresponds to a 1:1 ratio of MKC:SA and a 15 wt% catalyst amount added to the esterification reaction. At the lowest percentage of catalyst (5 wt%) with 1:1 of MKC:SA ratio, only about 69.5% oil removal was achieved. This shows that the oil removal efficiency of EKC was higher at 15 wt% than at 5 wt% catalyst. As reported in Section 3.2.2, the increase in catalyst amount allowed it to deprotonate more hydroxyl groups in the MKC structure, which eventually created



more SA attached to the MKC surface. In addition, a lower factor of MKC:SA ratio and a higher percentage of catalyst were required to facilitate the removal of oil from POME, as the combination of these terms (AB) has been proven to reduce the efficiency of the EKC.

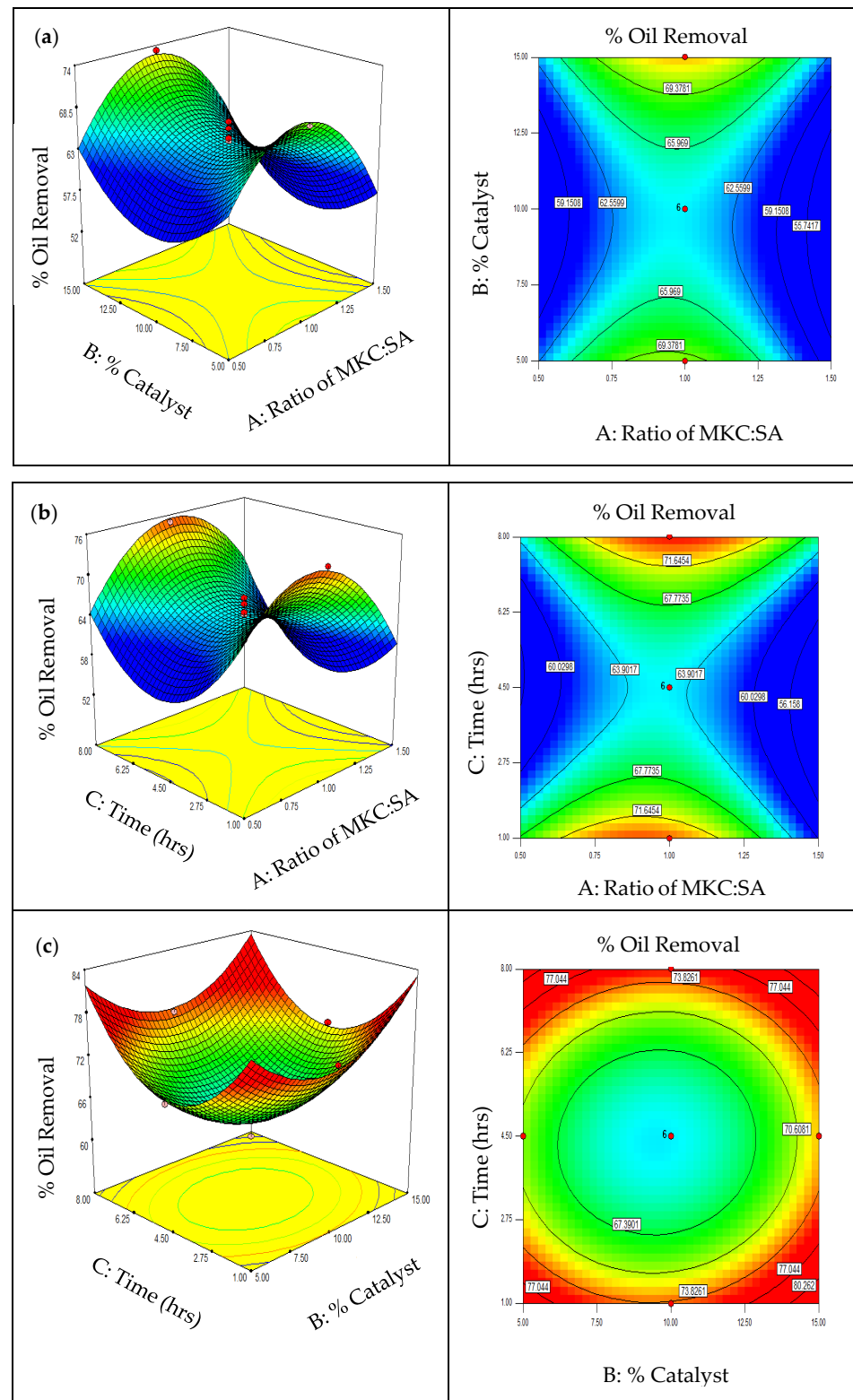


**Figure 7.** Response surface plots of the interaction effects of esterification factors on oil removal efficiency from POME: (a) ratio of RKC:SA and percentage of catalyst (AB), (b) ratio of RKC:SA and time (AC), and (c) percentage of catalyst and time (BC).

Meanwhile, Figure 7b illustrates the response surface plots of oil removal efficiency as a function of the MKC:SA ratio (A) and reflux time (C) at a fixed catalyst percentage (B) of 10 wt%. The shape of the surface plot obtained followed a trend similar to Figure 7a. The maximum oil removal efficiency of EKC was 74.9% at a 1:1 ratio of MKC:SA and 8 h reflux time (maximum duration). On the other hand, when the reflux time was reduced to 1 h (minimum duration), there was a slight difference in oil removal efficiency (74.7%) with the same ratio of MKC:SA (1:1). It was depicted that the increase in reflux time had a small significant effect on the removal of oil from POME, as the difference was only 0.2% when using 10 wt% catalyst in the esterification reaction. The increase in refluxing time has increased the fatty acid ester [80,81]. Based on this study, the increase in reflux time has increased the oil removal efficiency of EKC if the percentage of catalyst used is constant at 10 wt%. Thus, the combined effect of a lower ratio of MKC:SA (1:1) and a higher refluxing time (8 h) resulted in maximum oil removal efficiency using EKC.

Lastly, Figure 7c illustrates the response surface plots of oil removal efficiency as a function of catalyst percentage (B) and reflux time (C) at a constant ratio of MKC:SA (1:1). Based on the plot, at a 1 h reflux time, the oil removal efficiency of EKC using 5 wt% and 15 wt% of catalyst amount were 79% and 83%, respectively. However, as the reflux time increased to 8 h of operation, there was a slight increase in the oil removal efficiency of EKC. These corresponded to 82% and 83% of oil removal efficiency, recorded at the percentage catalyst of 5 wt% and 15 wt%, respectively. It was observed that the increase in catalyst percentage in the esterification reaction has increased the removal of oil from POME at both reflux times (1 h and 8 h). Nevertheless, it was noticeable that the higher reflux time gave a better oil removal efficiency from POME. The values of oil removal efficiency obtained were approximately close to each other, thus it can be concluded that 1 h is sufficient to conduct the reflux or esterification reaction due to economic factors. In fact, at 6 h reflux time and 15 wt% catalyst, a substantial amount of white solid SA residual covered half of the EKC surface. It was observed that the reaction at the highest reflux time (8 h) and the highest consumption of catalyst percentages (15 wt%) contributed the most enormous amount of white solid residual of SA and CaO, which fully covered the EKC surface. This was not observed under other reaction conditions in this study.

### 3.3.3. Optimization and Model Validation

The optimum condition for the oil removal efficiency of EKC was determined using numerical optimization, where the desirability value was used as an indicator. Ordinarily, the most optimum condition was suggested when the desirability value is equal to 1.0, which represents a completely desirable value or ideal response [82]. The response (oil removal efficiency) is usually calculated based on the independent factors at different combination levels set in CCD, according to the optimization goal of oil removal efficiency. Based on Table 4, the optimum conditions for maximum value of oil removal efficiency were predicted at the ratio of MKC to SA of 1:0.88 using 5.22% catalyst and a reflux time of 1.08 h. The predicted responses were attributed to 78.97% oil removal efficiency for EKC, corresponding to a desirability of 1.0. Thus, this implies that the predicted points were approximately acceptable compared to the observed response.

Meanwhile, the precision of the regression model displayed in the earlier section and the credibility of the optimum condition could be verified through the experimental work (run in triplicates), at the proposed optimum operating condition. As shown in Table 4, the experimental or observed response obtained was 72.4%, which fell between the 95% prediction intervals, namely within 72.85% (95% PI low) and 85.10% (95% PI high). Hence, the result obtained showed the suitability and validation of the quadratic polynomial model, and the regression model could be verified.

**Table 4.** Numerical optimization and model validation for oil removal efficiency from POME.

	Name	Optimization Goal	Lower Limit	Upper Limit	Prediction Point
<b>Factors</b>					
A	KC:SA ratio	Is in range	0.5	1.5	0.88
B	Percentage of catalyst (%)	Is in range	5	15	5.22
C	Refluxing time (hours)	Is in range	1	8	1.08
Response Y	Oil removal (%)	Maximum	60.5	76.0	78.97
Predicted response	Desirability	95% PI low	95% PI high	Observed response	
78.97	1.0	72.85	85.10	72.4	

### 3.3.4. Optimum Condition of Oil Removal Efficiency Using EKC as an Adsorbent to Remove Oil from POME

The experimental design for oil removal efficiency has been developed as described in Section 3.2, where the observed and predicted responses of the oil removal efficiency were tabulated in Table 2. The purpose of this study was to determine the optimum percentage of oil removal efficiency (Response) of EKC by conducting 18 experimental runs (all in triplicates) through the CCD analysis in RSM. The optimum condition to produce EKC with a maximum percentage of oil removal efficiency (76%) was a 1:0.5 ratio of MKC:SA, 15 wt% catalyst, and 1 h of reflux time. The maximum percentage of oil removal efficiency obtained for EKC was higher compared to RKC tested at the same dosage of 0.4 g, which achieved only 51% of oil removal efficiency. This shows that the mercerization and esterification reaction successfully increased the hydrophobicity and oil removal efficiency of RKC.

### 3.4. Case Study of Oil Adsorption Capacity

There are various factors controlling the oil adsorption process and the oil removal efficiency of an adsorbent. In a batch oil adsorption system, one of the key components that is remarkable in analyzing oil removal is the influence of solution pH. This is because the change in pH has an effect on the characteristics of the adsorbent surface, binding sites, and emulsion breaking [31,35,83]. The pH of the solution has a high impact on the emulsion stability by controlling the degree of ionization of the residual oil [35,84]. According to [64], different adsorbents would react differently toward the pH change during oil removal.

This study examined the influence of pH on the oil removal efficiency from POME for both RKC and EKC at pH levels of 2, 4.8, 7, and 8, as illustrated in Figure 8. This assessment highlights the impact of variations in pH on the adsorption efficacy of the materials. The analysis revealed that EKC consistently demonstrated higher oil removal efficiency than RKC. Both materials exhibited similar trends, with significantly higher removal efficiencies observed under acidic and basic conditions compared to neutral pH (7). However, EKC showed greater stability across the tested pH range due to the presence of ester groups, which enhanced its adsorption capacity for oil. The highest oil removal efficiencies for RKC and EKC were achieved at pH 2, with values of 76.8% and 91.4%, respectively. This improvement under strongly acidic conditions is attributed to the destabilization of oil droplets, leading to their increased size and easier adsorption onto the material surface. This phenomenon highlights the enhanced performance of both RKC and EKC under acidic conditions [9,31,35].

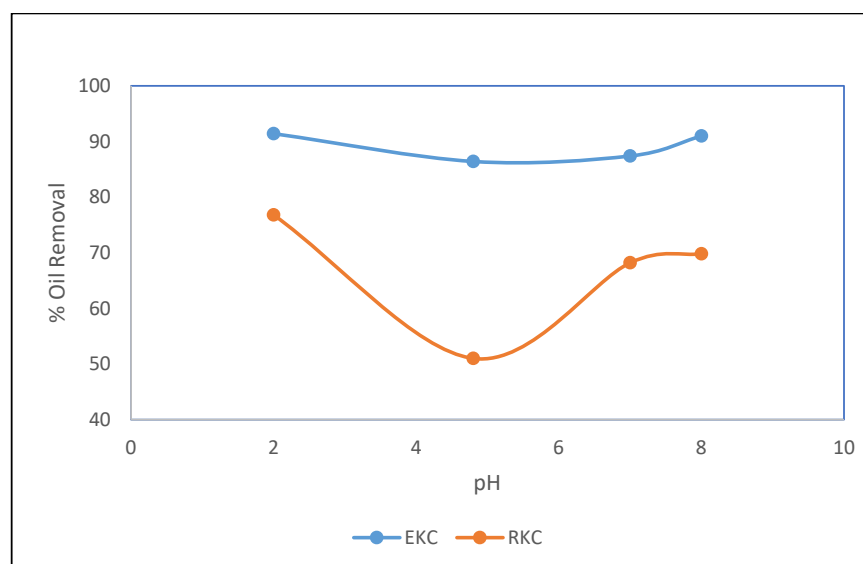


**Figure 8.** Effect of pH for RKC and EKC on oil removal from POME.

The lowest oil removal efficiency was observed at the original pH of POME (pH 4.8) for both RKC and EKC, with values of 51.0% and 86.4%, respectively. Beyond this point, the oil removal efficiency increased under strongly basic conditions, achieving 69.8% for RKC and 91.0% for EKC. However, the elevated removal efficiency at high pH levels was found to be inaccurate due to the saponification process. This process occurs when excessive NaOH is added to the POME solution, leading to the hydrolysis of residual oil into glycerol and fatty acid salts (soap), which are more soluble in water than in the organic solvent (n-hexane). This phenomenon, commonly observed with light and medium oils such as palm oil, can overstate the true adsorption efficiency of the materials.

While the maximum oil removal efficiency was attained under highly acidic circumstances (pH 2), it is noteworthy that the efficiency at the initial pH of POME (pH 4.8) was only slightly reduced (5%) for EKC. This finding highlights the importance of utilizing the original pH of POME for practical applications, as it obviates the necessity for substantial pH modifications while preserving high oil removal efficiency. Moreover, the enhanced efficacy of EKC as an oil adsorbent relative to RKC underscores the material's applicability in practical scenarios. These findings indicate the pivotal importance of pH in enhancing oil removal procedures and offer significant insights into the practical application of adsorption technology for POME treatment. Table 5 shows the comparison of percentage oil removal from POME using various adsorbents. The values of the percentage of oil removal for RKC and EKC are comparable with other types of adsorbents used in adsorbing the oil from POME.

**Table 5.** Comparison of oil removal percentages from POME using different adsorbents.

Adsorbent	Percentage of Oil Removal (%)	pH	Time (min)	Reference
RKC	76.8	2.0	30	This study
EKC	91.4	2.0	30	This study
Sago bark	48.2	2.0	30	[31]
Esterified sago bark	68.5	2.0	30	[31]
Natural zeolite	70.0	3.0	Not mentioned	[35]
Poly(dimethylsiloxane) (PDMS)	39.0	3.7		[83]
Carbon nanotubes (CNT's)—PDMS	64.0	3.7		[83]

### 3.5. Characterization

#### 3.5.1. Attenuated Total Reflectance—Fourier Transform Infrared Spectroscopy (ATR-FTIR)

ATR-FTIR analysis was carried out to characterize the functional group that is present before and after the esterification reaction. Figure 9 presents the FTIR spectra for these samples, highlighting significant changes following esterification and subsequent oil adsorption. The FTIR spectra of RKC revealed key peaks at  $3854\text{ cm}^{-1}$ ,  $3813\text{ cm}^{-1}$ ,  $3748\text{ cm}^{-1}$ ,  $3460\text{ cm}^{-1}$ , and  $3025\text{ cm}^{-1}$ , corresponding to O-H stretching, C=C stretching of ketone ( $2326\text{ cm}^{-1}$ ), and C=O stretching of ester ( $1747\text{ cm}^{-1}$ ) in the cellulosic fiber. This indicates the presence of hydroxyl groups and native ester bonds inherent to RKC. Following esterification, the FTIR spectra of EKC showed a notable reduction in the O-H peak intensity compared to RKC, confirming the successful replacement of hydroxyl groups with ester groups [37,48,64]. This transformation is further validated by the shift in the C=O ester peak from  $1747\text{ cm}^{-1}$  in RKC to  $1735\text{ cm}^{-1}$  in EKC, indicating the formation of ester bonds. The presence of these ester groups is pivotal, as they impart hydrophobicity to EKC, facilitating oil adsorption from POME [24,64,85].

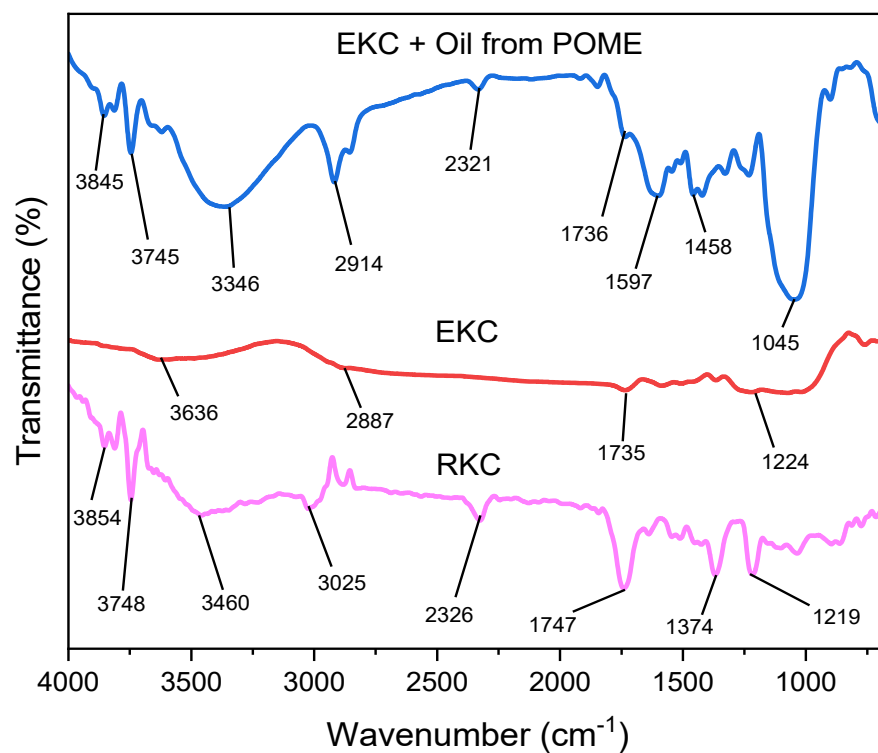


**Figure 9.** FTIR spectra of RKC, EKC, and EKC after oil adsorption from POME.

After oil adsorption, the FTIR spectra of EKC demonstrated several distinctive changes. The spectral range between  $3845$  and  $3346\text{ cm}^{-1}$  exhibited peaks attributable to O-H stretching groups, which likely originated from hydroxyl groups attached to hydrocarbon chains within the oil mixture. A significant new peak at  $2914\text{ cm}^{-1}$  was observed, confirming the presence of C-H stretching vibrations associated with aliphatic hydrocarbons, a major component of oils [84]. Notably, peaks corresponding to C=C stretching of aromatic hydrocarbons ( $1597\text{ cm}^{-1}$ ) and C-H bending vibrations ( $1458\text{ cm}^{-1}$ ) appeared in the EKC spectra post-adsorption, providing further evidence of oil attachment to the EKC surface [44,86]. Additionally, a prominent peak at  $1045\text{ cm}^{-1}$  indicated C-O bending vibrations in primary alcohols, alongside the hydrogen-bonded O-H stretching at  $3346\text{ cm}^{-1}$  [87]. The decrease in intensity of the ester peak ( $1736\text{ cm}^{-1}$ ) in EKC after oil adsorption, compared to RKC and untreated EKC, suggests strong interactions between the ester groups and the oil molecules.



This observation further supports the role of ester groups in capturing and binding oil to the EKC surface. FTIR analysis demonstrates the successful modification of RKC into EKC via esterification, enhancing its hydrophobic nature for efficient oil adsorption. The spectral changes observed after oil adsorption confirm the presence of aliphatic hydrocarbons, aromatic C=C bonds, and functional groups from the adsorbed oil, providing strong evidence of EKC's efficacy as an oil adsorbent.

### 3.5.2. Scanning Electron Microscopy (SEM)

The surface morphology of RKC and EKC was examined using scanning electron microscopy (SEM) to observe the structural changes resulting from mercerization and esterification treatments. Figure 10 presents the SEM micrographs of RKC at two different magnifications: 100 $\times$  (Figure 10a) and 600 $\times$  (Figure 10b). At 100 $\times$  magnification, the surface of RKC exhibited relatively smooth and irregular textures, with only minor pores visible (shown in yellow arrow in Figure 10a). The smoothness of the surface is attributed to the natural waxes and oils present in the lignocellulosic fibers of RKC, which coat the surface [88]. When magnified to 600 $\times$ , a more detailed view reveals the presence of rigid, open cylindrical pores with an irregular distribution (Figure 10b). Furthermore, impurities, marked with yellow arrows in Figure 10b, were detected on the RKC surface. These impurities likely originated from the salt (NaCl) used in the pulping process, where sodium ions ( $\text{Na}^+$ ) from sodium hydroxide (NaOH) react with chloride ions ( $\text{Cl}^-$ ) from hydrochloric acid (HCl) during acid precipitation [89].

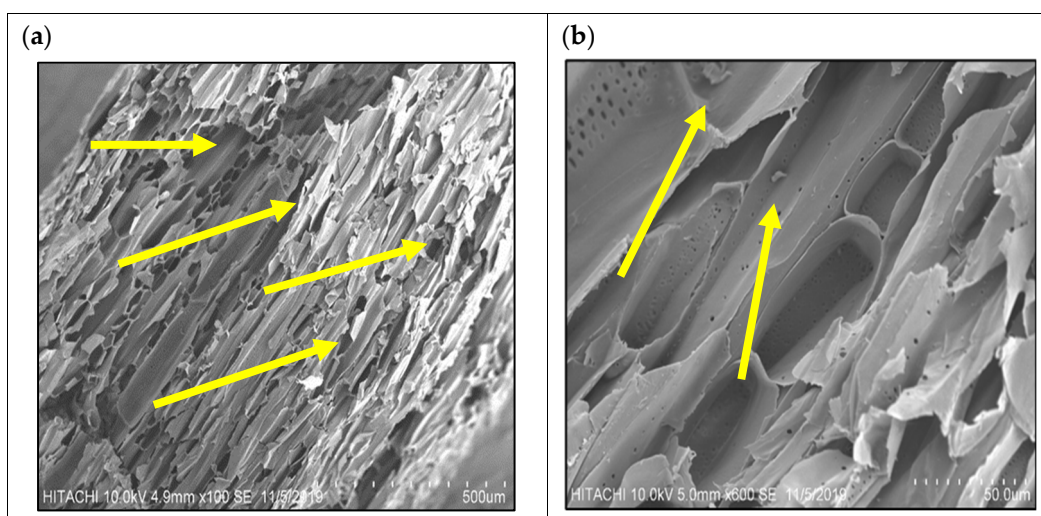


**Figure 10.** SEM micrograph of RKC at (a) 100 $\times$  and (b) 600 $\times$  magnifications.

Following mercerization and esterification, the surface morphology of EKC showed more pronounced changes. Figure 11 presents the SEM micrographs of EKC at 100 $\times$  magnification. The surface exhibited increased porosity, with more pores developed compared to RKC (indicated by arrows in Figure 11a). Additionally, the cross-sectional image in Figure 11b revealed the formation of internal pores within the EKC structure. The mercerization process notably increased the surface roughness, contributing to a larger surface area [90,91]. These rough and porous characteristics are crucial for enhancing the oil adsorption capacity of EKC, making it more efficient at capturing oil from POME. The increased surface area provides more active sites for oil adsorption, improving interfacial bonding between the oil and the EKC surface [24,90,92,93].



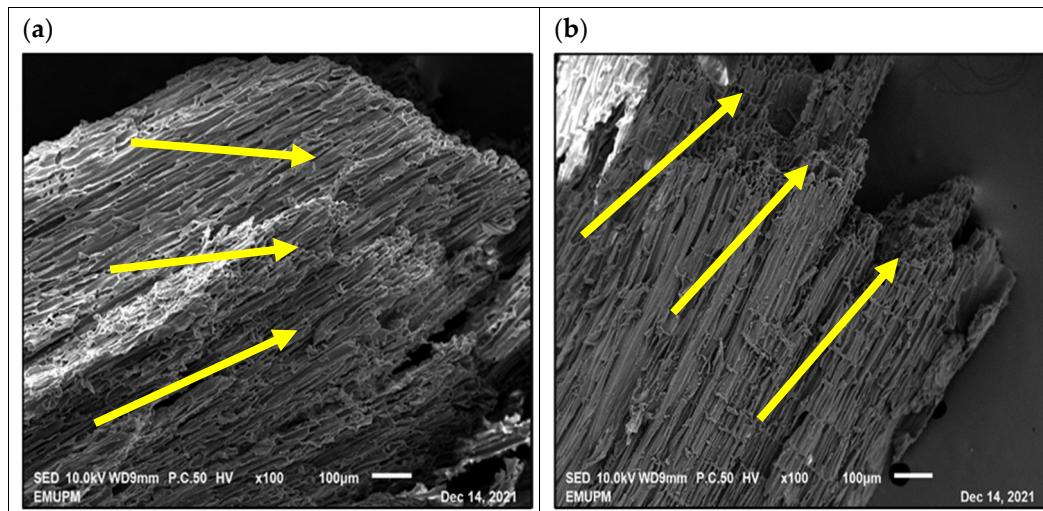


**Figure 11.** SEM micrograph of EKC using 100 $\times$  magnification. (a) A rougher texture was noticeable on the EKC surface. (b) Cross-section image of EKC.

At 600 $\times$  magnification, Figure 12 provides a closer view of EKC's surface after mercerization and esterification. More uniform pores are evident (indicated by arrows in Figure 12a), with the pores aligned in a honeycomb structure (Figure 12b). This formation of heterogeneous pores is attributed to the expansion of smaller interior pores in the fibers and fibrils, resulting from the alkaline treatment with NaOH during mercerization [94]. These open cylindrical pores and perforations offer excellent sites for oil adsorption, as they provide a larger surface area for oil to be trapped and retained on the EKC surface [95].

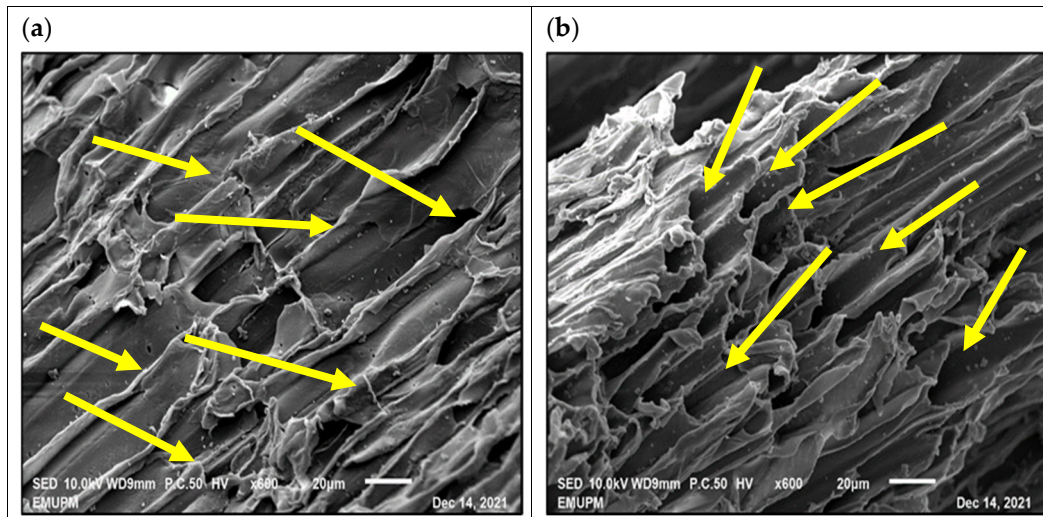


**Figure 12.** SEM micrograph of EKC using 600 $\times$  magnification. (a) More uniform pores were visible on the EKC surface. (b) Pores were aligned in a heterogeneous pore group of honeycomb structure.

In addition to the pore formation, fibrillation on the EKC surface was observed, likely due to the mechanical disruption of fibers during the mercerization process [91,96]. The presence of CaO in the esterification reaction is also thought to contribute to fibrillation [33]. Furthermore, mercerization effectively cleaned the fibers, removed impurities, and enhanced the surface properties of EKC [88]. The SEM analysis reveals significant morphological transformations in EKC after mercerization and esterification. The development of a rougher texture, increased porosity, and the formation of a honeycomb pore structure significantly enhance the adsorption capacity of EKC for oil from POME. These

structural changes, including the expansion of fibrils and removal of impurities, are critical for improving the interfacial interaction between the oil and the EKC surface, thereby increasing the overall oil removal efficiency.

#### 4. Conclusions

This research reveals the effective modification of raw kenaf core (RKC) fiber via mercerization and esterification, enhancing its hydrophobic properties and oil extraction efficacy for palm oil mill effluent (POME) remediation. The mercerization process revealed more hydroxyl groups on the mercerized kenaf core (MKC) fiber surface, which then reacted with stearic acid (SA) during esterification to produce ester groups, thereby markedly enhancing its surface hydrophobicity. A regression model with an  $R^2$  value of 0.94 determined the optimum parameters for oil removal as a 1:0.5 MKC:SA ratio, 15 wt% catalyst, and a reflux duration of 1 h, resulting in a 76% oil removal efficiency, in contrast to 51% with untreated RKC. The case study revealed that the highest oil adsorption capacity was obtained in acidic conditions for both RKC and EKC, compared to alkali and neutral conditions. However, EKC exhibited a higher adsorption capacity compared to RKC, demonstrating that EKC has the potential to become a good oil adsorbent. FTIR research affirmed the effective production of esters and the reduction of hydroxyl groups, while SEM imaging demonstrated enhanced surface roughness, fibrillation, and porosity in the modified cellulose, leading to improved oil adsorption. The findings indicate that EKC is an effective and economical adsorbent for oil extraction from POME, with the potential for future optimization via batch studies and kinetic modeling to assess its full industrial applicability.

**Author Contributions:** Conceptualization, N.H.A., L.C.A. and S.N.A.M.J.; methodology, N.H.A.; software, N.H.A.; validation, N.H.A. and L.C.A.; formal analysis, N.H.A.; investigation, N.H.A.; writing—original draft preparation, N.H.A.; writing—review and editing, N.H.A., L.C.A., C.L.L. and A.A.A.; supervision, L.C.A., T.C.S.Y., S.N.A.M.J., T.M.T. and A.J.A.; funding acquisition, L.C.A. and A.J.A. All authors have read and agreed to the published version of the manuscript.

**Funding:** This research received no external funding.

**Data Availability Statement:** The original contributions presented in this study are included in the article. Further inquiries can be directed to the corresponding authors.

**Acknowledgments:** The authors would like to thank the Department of Chemical and Environmental Engineering, Faculty of Engineering, Universiti Putra Malaysia, Serdang, Selangor, Malaysia, for providing research amenities for this project and Sime Darby Research Sdn. Bhd. and School of Chemical Engineering, College of Engineering, Universiti Teknologi MARA, Shah Alam, Selangor, Malaysia, for financial support.

**Conflicts of Interest:** Ahmad Jaril Asis was employed by Sime Darby Research Sdn. Bhd.; the remaining authors declare that the research was conducted in the absence of any commercial or financial relationships that could be construed as a potential conflict of interest.

#### References

1. Adetunji, A.I.; Olaniran, A.O. Treatment of Industrial Oily Wastewater by Advanced Technologies: A Review. *Appl. Water Sci.* **2021**, *11*, 1–19. [[CrossRef](#)]
2. Jamaly, S.; Giwa, A.; Hasan, S.W. Recent Improvements in Oily Wastewater Treatment: Progress, Challenges, and Future Opportunities. *J. Environ. Sci.* **2015**, *37*, 15–30. [[CrossRef](#)] [[PubMed](#)]
3. Wei, Y.; Jin, Y.; Zhang, W. Treatment of High-Concentration Wastewater from an Oil and Gas Field via a Paired Sequencing Batch and Ceramic Membrane Reactor. *Int. J. Environ. Res. Public Health* **2020**, *17*, 1953. [[CrossRef](#)] [[PubMed](#)]
4. Wang, Y.; Zhang, Y.; Liang, L.; Tu, F.; Li, Z.; Tang, X.; Dai, L.; Li, L. Research Progress on Membrane Separation Technology for Oily Wastewater Treatment. *Toxics* **2024**, *12*, 794. [[CrossRef](#)] [[PubMed](#)]

5. Abuhasel, K.; Kchaou, M.; Alquraish, M.; Munusamy, Y.; Jeng, Y.T. Oilywastewater Treatment: Overview of Conventional and Modern Methods, Challenges, and Future Opportunities. *Water* **2021**, *13*, 980. [[CrossRef](#)]
6. de Medeiros, A.D.M.; da Silva Junior, C.J.G.; de Amorim, J.D.P.; Durval, I.J.B.; de Santana Costa, A.F.; Sarubbo, L.A. Oily Wastewater Treatment: Methods, Challenges, and Trends. *Processes* **2022**, *10*, 743. [[CrossRef](#)]
7. Haan, T.Y.; Isma Nordin, P.M.; Ahmad Juanda, N.T.; Mohd Shafi, M.A.; Krishnan, P. A Review on Adsorption Process for the Treatment of Oily Wastewater. *Adv. Environ. Eng. Res.* **2023**, *4*, 1–21. [[CrossRef](#)]
8. Ramli, A.N.; Mohd Ghazi, R. Removal of Oil and Grease in Wastewater Using Palm Kernel Shell Activated Carbon. In *IOP Conference Series: Earth and Environmental Science, Proceedings of the 2nd International Conference on Tropical Resources and Sustainable Sciences Pengkalan Chepa, Malaysia, 10–11 August 2020*; IOP Publishing Ltd.: Bristol, UK, 2020; Volume 549.
9. Ahmad, A.L.; Sumathi, S.; Hameed, B.H. Adsorption of Residue Oil from Palm Oil Mill Effluent Using Powder and Flake Chitosan: Equilibrium and Kinetic Studies. *Water Res.* **2005**, *39*, 2483–2494. [[CrossRef](#)]
10. Madaki, Y.S.; Seng, L. Palm Oil Mill Effluent (POME) from Malaysia Palm Oil Mills: Waste or Resource. *Int. J. Sci. Environ.* **2013**, *2*, 1138–1155.
11. Liew, R.K.; Chai, C.; Yek, P.N.Y.; Phang, X.Y.; Chong, M.Y.; Nam, W.L.; Su, M.H.; Lam, W.H.; Ma, N.L.; Lam, S.S. Innovative Production of Highly Porous Carbon for Industrial Effluent Remediation via Microwave Vacuum Pyrolysis plus Sodium-Potassium Hydroxide Mixture Activation. *J. Clean. Prod.* **2019**, *208*, 1436–1445. [[CrossRef](#)]
12. Ma, A.N. Environmental Management for the Palm Oil Industry. *Palm Oil Dev.* **2000**, *30*, 1–10.
13. Ahmad, A.L.; Bhatia, S.; Ibrahim, N.; Sumathi, S. Adsorption of Residual Oil from Palm Oil Mill Effluent Using Rubber Powder. *Braz. J. Chem. Eng.* **2005**, *22*, 371–379. [[CrossRef](#)]
14. Igwe, J.C.; Onyegbado, C.C. A Review of Palm Oil Mill Effluent (Pome) Water Treatment. *Glob. J. Environ. Res.* **2007**, *1*, 54–62.
15. Zinatizadeh, A.A.L.; Salamatinia, B.; Mohamed, A.R.; Isa Hasnain, M. Palm Oil Mill Effluent Digestion in an Up-Flow Anaerobic Sludge Fixed Film Bioreactor. *Int. J. Environ. Res.* **2007**, *1*, 264–271.
16. Chan, Y.J.; Chong, M.F.; Law, C.L. An Integrated Anaerobic-Aerobic Bioreactor (IAAB) for the Treatment of Palm Oil Mill Effluent (POME): Start-up and Steady State Performance. *Process Biochem.* **2012**, *47*, 485–495. [[CrossRef](#)]
17. Khemkhao, M.; Nuntakumjorn, B.; Techkarnjanaruk, S.; Phalakornkule, C. UASB Performance and Microbial Adaptation during a Transition from Mesophilic to Thermophilic Treatment of Palm Oil Mill Effluent. *J. Environ. Manag.* **2012**, *103*, 74–82. [[CrossRef](#)] [[PubMed](#)]
18. Zaied, B.K.; Nasrullah, M.; Islam Siddique, M.N.; Zularisam, A.W.; Singh, L.; Krishnan, S. Enhanced Bioenergy Production from Palm Oil Mill Effluent by Co-Digestion in Solar Assisted Bioreactor: Effects of Hydrogen Peroxide Pretreatment. *J. Environ. Chem. Eng.* **2020**, *8*, 1–29. [[CrossRef](#)]
19. Lee, M.D.; Lee, P.P. Performance of Chitosan as Natural Coagulant in Oil Palm Mill Effluent Treatment. In *Promising Techniques for Wastewater Treatment and Water Quality Assessment*; IntechOpen: London, UK, 2020; pp. 1–21.
20. Wu, T.Y.; Mohammad, A.W.; Md Jahim, J.; Anuar, N. Pollution Control Technologies for the Treatment of Palm Oil Mill Effluent (POME) through End-of-Pipe Processes. *J. Environ. Manag.* **2010**, *91*, 1467–1490. [[CrossRef](#)] [[PubMed](#)]
21. Jadhav, P.; Muhammad, N.; Bhuyar, P.; Krishnan, S.; Abd Razak, A.S.; Zularisam, A.W.; Nasrullah, M. A Review on the Impact of Conductive Nanoparticles (CNPs) in Anaerobic Digestion: Applications and Limitations. *Environ. Technol. Innov.* **2021**, *23*, 1–16. [[CrossRef](#)]
22. Saad, M.S.; Joe, N.G.; Shuib, H.A.; Hakim Wirzal, M.D.; Adi Putra, Z.; Khan, M.R.; Busquets, R. Techno-Economic Analysis of an Integrated Electrocoagulation-Membrane System in Treatment of Palm Oil Mill Effluent. *J. King Saud. Univ. Sci.* **2022**, *34*, 1–10. [[CrossRef](#)]
23. Adeleke, O.A.; Ismail, N.; Fadilat, A.; Apandi, N.; Latiff, A.A.A.; Saphira, M.R.; Daud, Z.; Ab Aziz, N.A.; Al-Gheethi, A.; Kumar, V.; et al. Principles and Mechanism of Adsorption for the Effective Treatment of Palm Oil Mill Effluent for Water Reuse. In *Nanotechnology in Water and Wastewater Treatment: Theory and Applications*; Elsevier: Amsterdam, The Netherlands, 2019; pp. 1–33. ISBN 9780128139028.
24. Alias, N.H.; Abdullah, L.C.; Choong, T.S.Y.; Md Jamil, S.N.A.; Asis, A.J.; Rusli, N.H. Oil Removal From Palm Oil Mill Effluent (POME) by Using Kenaf Core (*Hibiscus cannabinus*). *Adv. Eng. Res.* **2020**, *200*, 158–163.
25. Ahmad, A.L.; Sithamparam, K.; Ismail, S. Extraction of Residual Oil from Palm Oil Mill Effluent (POME) Using Organic Solvent. *ASEAN J. Sci. Technol. Dev.* **2003**, *20*, 385–394. [[CrossRef](#)]
26. Ahmad, A.L.; Bhatia, S.; Ibrahim, N.; Ismail, S. Coagulation-Sedimentation-Extraction Pretreatment Methods for the Removal of Suspended Solids and Residual Oil from Palm Oil Mill Effluent (POME). *IIUM Eng. J.* **2002**, *3*, 25–33.
27. Laohaprapanon, T.; Prasertsan, P.; Kittikun, A.H. Physical and Chemical Separation of Oil and Suspended Solids from Palm Oil Mill Effluent. *Asian J. Energy Environ.* **2005**, *6*, 39–55.
28. Ang, W.L.; Mohammad, A.W. State of the Art and Sustainability of Natural Coagulants in Water and Wastewater Treatment. *J. Clean. Prod.* **2020**, *262*, 1–18. [[CrossRef](#)]



29. Sánchez-Martín, J.; Ghebremichael, K.; Beltrán-Heredia, J. Comparison of Single-Step and Two-Step Purified Coagulants from Moringa Oleifera Seed for Turbidity and DOC Removal. *Bioresour. Technol.* **2010**, *101*, 6259–6261. [CrossRef]
30. Pintor, A.M.A.; Vilar, V.J.P.; Botelho, C.M.S.; Boaventura, R.A.R. Oil and Grease Removal from Wastewaters: Sorption Treatment as an Alternative to State-of-the-Art Technologies. A Critical Review. *Chem. Eng. J.* **2016**, *297*, 229–255. [CrossRef]
31. Wahi, R.; Chuah Abdullah, L.; Nourouzi Mobarekeh, M.; Ngaini, Z.; Choong Shean Yaw, T. Utilization of Esterified Sago Bark Fibre Waste for Removal of Oil from Palm Oil Mill Effluent. *J. Environ. Chem. Eng.* **2017**, *5*, 170–177. [CrossRef]
32. Stawiński, W.; Węgrzyn, A.; Dańko, T.; Freitas, O.; Figueiredo, S.; Chmielarz, L. Acid-Base Treated Vermiculite as High Performance Adsorbent: Insights into the Mechanism of Cationic Dyes Adsorption, Regeneration, Recyclability and Stability Studies. *Chemosphere* **2017**, *173*, 107–115. [CrossRef] [PubMed]
33. Wahi, R.; Abdullah, L.C.; Ngaini, Z.; Nourouzi, M.M.; Choong, T.S.Y. Esterification of M. Sagu Bark as an Adsorbent for Removal of Emulsified Oil. *J. Environ. Chem. Eng.* **2014**, *2*, 324–331. [CrossRef]
34. Mohd Nawawi, M.G.; Othman, N.; Sadikin, A.N.; Khalid, S.S.; Yusof, N. Development of Empty Fruit Bunch Filter with Addition of Chitosan for Pre-Treatment of Palm Oil Mill Effluent. *J. Chem. Nat. Resour. Eng.* **2008**, *2*, 8–16.
35. Shavandi, M.A.; Haddadian, Z.; Ismail, M.H.S.; Abdullah, N.; Abidin, Z.Z. Removal of Residual Oils from Palm Oil Mill Effluent by Adsorption on Natural Zeolite. *Water Air Soil. Pollut.* **2012**, *223*, 4017–4027. [CrossRef]
36. Viju, S.; Thilagavathi, G.; Vignesh, B.; Brindha, R. Oil Sorption Behavior of Acetylated Nettle Fiber. *J. Text. Inst.* **2019**, *110*, 1415–1423. [CrossRef]
37. Asadpour, R.; Sapari, N.; Isa, M.H.; Orji, K.U. Investigation of Modified Mangrove Bark on the Sorption of Oil in Water. *Appl. Mech. Mater.* **2014**, *567*, 74–79. [CrossRef]
38. Asadpour, R.; Yavari, S.; Kamyab, H.; Ashokkumar, V.; Chelliapan, S.; Yuzir, A. Study of Oil Sorption Behaviour of Esterified Oil Palm Empty Fruit Bunch (OPEFB) Fibre and Its Kinetics and Isotherm Studies. *Environ. Technol. Innov.* **2021**, *22*, 1–12. [CrossRef]
39. Zamparas, M.; Tzivras, D.; Dracopoulos, V.; Ioannides, T. Application of Sorbents for Oil Spill Cleanup Focusing on Natural-Based Modified Materials: A Review. *Molecules* **2020**, *25*, 4522. [CrossRef]
40. Teli, M.D.; Valia, S.P. Grafting of Butyl Acrylate on to Banana Fibers for Improved Oil Absorption. *J. Nat. Fibers* **2016**, *13*, 470–476. [CrossRef]
41. Asadpour, R.; Sapari, N.; Isa, M.H.; Orji, K.U. Enhancing the Hydrophobicity of Mangrove Bark by Esterification for Oil Adsorption. *Water Sci. Technol.* **2014**, *70*, 1220–1228. [CrossRef]
42. Jahi, N.; Othaman, R.; Lazim, A.M.; Ramli, S. Empty Fruit Bunch Cellulose Based Sorbent for Oil Sorption in Palm Oil Mill Effluent. *Sains Malays.* **2020**, *49*, 2323–2333. [CrossRef]
43. Jawad, R.J.; Ismail, M.H.S.; Siajam, S.I. Adsorption of Heavy Metals and Residual Oil from Palm Oil Mill Effluent Using a Novel Adsorbent of Alginate and Mangrove Composite Beads Coated with Chitosan in a Packed Bed Column. *IJUM Eng. J.* **2018**, *19*, 1–14. [CrossRef]
44. Jahi, N.; Ling, E.S.; Othaman, R.; Ramli, S. Modification of Oil Palm Plantation Wastes as Oil Adsorbent for Palm Oil Mill Effluent (POME). *Malays. J. Anal. Sci.* **2015**, *19*, 31–40.
45. Ngarmkam, W.; Sirisathitkul, C.; Phalakornkule, C. Magnetic Composite Prepared from Palm Shell-Based Carbon and Application for Recovery of Residual Oil from POME. *J. Environ. Manag.* **2011**, *92*, 472–479. [CrossRef] [PubMed]
46. Ekwueme, B.N.; Ezema, C.A.; Asadu, C.O.; Onu, C.E.; Onah, T.O.; Ike, I.S.; Orga, A.C. Isotherm Modelling and Optimization of Oil Layer Removal from Surface Water by Organic Acid Activated Plantain Peels Fiber. *Arab. J. Chem.* **2023**, *16*, 1–19. [CrossRef]
47. Sathasivam, K.; Mas Haris, M.R.H. Adsorption Kinetics and Capacity of Fatty Acid-Modified Banana Trunk Fibers for Oil in Water. *Water Air Soil. Pollut.* **2010**, *213*, 413–423. [CrossRef]
48. Banerjee, S.S.; Joshi, M.V.; Jayaram, R.V. Treatment of Oil Spill by Sorption Technique Using Fatty Acid Grafted Sawdust. *Chemosphere* **2006**, *64*, 1026–1031. [CrossRef] [PubMed]
49. Crane, J.C. Kenaf Fiber-Plant Rival of Jute 1. *Econ. Bot.* **1947**, *1*, 334–350. [CrossRef]
50. Saba, N.; Jawaid, M.; Hakeem, K.R.; Paridah, M.T.; Khalina, A.; Alothman, O.Y. Potential of Bioenergy Production from Industrial Kenaf (*Hibiscus cannabinus* L.) Based on Malaysian Perspective. *Renew. Sustain. Energy Rev.* **2015**, *42*, 446–459. [CrossRef]
51. Wilson, F.D.; Menzel, M.Y. Kenaf (*Hibiscus cannabinus*), Roselle (*Hibiscus sabdariffa*). *Econ. Bot.* **1964**, *18*, 80–91. [CrossRef]
52. Anonymous Kenaf: GOVT to Expand Kenaf Cultivation Nationwide. Available online: <https://www.bernama.com/en/news.php?id=1868782> (accessed on 23 January 2025).
53. Tan, J.Y.; Low, S.Y.; Ban, Z.H.; Siwayanan, P. A Review on Oil Spill Clean-up Using Bio-Sorbent Materials with Special Emphasis on Utilization of Kenaf Core Fibres. *Bioresources* **2021**, *16*, 8394–8416. [CrossRef]
54. Kujoana, T.C.; Weeks, W.J.; Van der Westhuizen, M.M.; Mabelebele, M.; Sebola, N.A. Potential Significance of Kenaf (*Hibiscus Cannabinus* L.) to Global Food and Feed Industries. *Cogent Food Agric.* **2023**, *9*, 1–16. [CrossRef]
55. Hayemasae, N.; Viet, C.X.; Masa, A.; Shuib, R.K.; Ismail, H.; Surya, I. The Use of Kenaf Fibre as a Natural Anti-Degradant in Recycled High-Density Polyethylene and Natural Rubber-Based Thermoplastic Elastomers. *Polymers* **2023**, *15*, 1–16. [CrossRef] [PubMed]

56. Sajab, M.S.; Chia, C.H.; Zakaria, S.; Mohd Jani, S.; Khiew, P.S.; Chiu, W.S. Removal of Copper(II) Ions from Aqueous Solution Using Alkali-Treated Kenaf Core Fibres. *Adsorpt. Sci. Technol.* **2010**, *28*, 377–386. [CrossRef]
57. Sajab, M.S.; Chia, C.H.; Zakaria, S.; Jani, S.M.; Ayob, M.K.; Chee, K.L.; Khiew, P.S.; Chiu, W.S. Citric Acid Modified Kenaf Core Fibres for Removal of Methylene Blue from Aqueous Solution. *Bioresour. Technol.* **2011**, *102*, 7237–7243. [CrossRef] [PubMed]
58. Anonymous Coal. Available online: <https://tradingeconomics.com/commodity/coal> (accessed on 23 January 2025).
59. Quora, Inc. Why Are Fatty Acids Hydrophobic? Available online: <https://www.quora.com/Why-are-fatty-acids-hydrophobic> (accessed on 16 July 2021).
60. Stat-Ease, Inc. Design-Expert V22.0: Anova Output. Available online: <https://www.statease.com/docs/latest/contents/analysis/anova-output/> (accessed on 5 December 2022).
61. Clesceri, L.S.; Greenberg, A.E.; Eaton, A.D. *Standard Methods for the Examination of Water and Wastewater*, 20th ed.; APHA, AWWA, WEF: Washington, CD, USA, 1999.
62. RTI Laboratories FTIR Analysis | RTI Laboratories. Available online: <https://rtilab.com/techniques/ftir-analysis/> (accessed on 23 May 2018).
63. Laboratory Testing Inc. Scanning Electron Microscopy, SEM Analysis. Available online: <https://www.labtesting.com/services/materials-testing/metallurgical-testing/sem-analysis/> (accessed on 26 May 2018).
64. Wahi, R. Application of Esterified Sago Bark for Removal of Oil from Palm Oil Mill Effluent. Ph.D. Thesis, Universiti Putra Malaysia, Serdang, Selangor, Malaysia, 2014.
65. Satriadi, H.; Khaibar, A.; Almakhi, M.M. Biodiesel Production by Using Heterogeneous Catalyst from Fly Ash and Limestone. In Proceedings of the 2017 International Conference on Sustainable Energy Engineering and Application (ICSEEA), Jakarta, Indonesia, 23–24 October 2017; pp. 41–44.
66. Hadiyanto, H.; Lestari, S.P.; Abdullah, A.; Widayat, W.; Sutanto, H. The Development of Fly Ash-Supported CaO Derived from Mollusk Shell of Anadara Granosa and Paphia Undulata as Heterogeneous CaO Catalyst in Biodiesel Synthesis. *Int. J. Energy Environ. Eng.* **2016**, *7*, 297–305. [CrossRef]
67. Basumatary, S.F.; Brahma, S.; Hoque, M.; Das, B.K.; Selvaraj, M.; Brahma, S.; Basumatary, S. Advances in CaO-Based Catalysts for Sustainable Biodiesel Synthesis. *Green. Energy Resour.* **2023**, *1*, 1–31. [CrossRef]
68. Wong, Y.C.; Tan, Y.P.; Taufiq-Yap, Y.H.; Ramli, I. Effect of Calcination Temperatures of CaO/Nb<sub>2</sub>O<sub>5</sub> Mixed Oxides Catalysts on Biodiesel Production (Kesan Suhu Pengkalsinan Oksida Campuran CaO/Nb<sub>2</sub>O<sub>5</sub> Ke Atas Penghasilan Biodiesel). *Sains Malaysiana.* **2014**, *43*, 783–790.
69. Abd Aziz, A.S. *The Basics of Chemical Plant Operations*, 1st ed.; Azharin Shah bin Abd Aziz: Kemaman, Malaysia, 2023; ISBN 978-629-99043-0-4.
70. Saha, R.; Goud, V.V. Ultrasound Assisted Transesterification of High Free Fatty Acids Karanja Oil Using Heterogeneous Base Catalysts. *Biomass Convers. Biorefin* **2015**, *5*, 195–207. [CrossRef]
71. Abu Bakar, N.N.; Latip, J.; Sopian, S.; Mohd Khalid, R. Optimization of Roselle (*Hibiscus sabdariffa* Linn.) Anthocyanin Extraction Parameter by Response Surface Modeling and Potential of Roselle Agro-Waste as Alternative Sources of Anthocyanin. *Sains Malays.* **2023**, *52*, 3147–3162. [CrossRef]
72. Madhumita, M.; Guha, P.; Nag, A. Extraction of Betel Leaves (*Piper betle* L.) Essential Oil and Its Bio-Actives Identification: Process Optimization, GC-MS Analysis and Anti-Microbial Activity. *Ind. Crops Prod.* **2019**, *138*, 1–12. [CrossRef]
73. Samadi, M.; Zainal Abidin, Z.; Yoshida, H.; Yunus, R.; Awang Biak, D.R.; Lee, C.H.; Lok, E.H. Subcritical Water Extraction of Essential Oil from Aquilaria Malaccensis Leaves. *Sep. Sci. Technol.* **2020**, *55*, 2779–2798. [CrossRef]
74. Anderson, M.J.; Whitcomb, P.J. *Anderson\_Whitcomb 2017 RSM-Optimizing Processes Using. Response Surface Methods for Design of Experiments*, 2nd ed.; CRC Press, Taylor & Francis Group: Boca Raton, FL, USA, 2017; ISBN 978-1-4987-4598-7.
75. Frost, J. Statistics by Jim: How To Interpret R-Squared in Regression Analysis. Available online: <https://statisticsbyjim.com/regression/interpret-r-squared-regression/> (accessed on 11 March 2023).
76. Zhang, L.; Cheng, Z.; Guo, X.; Jiang, X.; Liu, R. Process Optimization, Kinetics and Equilibrium of Orange G and Acid Orange 7 Adsorptions onto Chitosan/Surfactant. *J. Mol. Liq.* **2014**, *197*, 353–367. [CrossRef]
77. Yu, P.; Chao, X. Statistics-Based Optimization of the Extraction Process of Kelp Polysaccharide and Its Activities. *Carbohydr. Polym.* **2013**, *91*, 356–362. [CrossRef] [PubMed]
78. Prakash Maran, J.; Manikandan, S. Response Surface Modeling and Optimization of Process Parameters for Aqueous Extraction of Pigments from Prickly Pear (*Opuntia Ficus-Indica*) Fruit. *Dye. Pigment.* **2012**, *95*, 465–472. [CrossRef]
79. The Pennsylvania State University 4.6-Normally Probability Plot of Residuals. Available online: <https://online.stat.psu.edu/stat501/lesson/4/4.6> (accessed on 16 March 2023).
80. Burmana, A.D.; Tambun, R.; Haryanto, B.; Alexander, V. Effect of Reaction Time on Biodiesel Production from Palm Fatty Acid Distillate by Using PTSA as a Catalyst. In *IOP Conference Series: Materials Science and Engineering, Proceedings of the 2nd International Conference on Industrial and Manufacturing Engineering (ICI&ME 2020), Medan, Indonesia, 3–4 September 2020*; IOP Publishing Ltd.: Bristol, UK, 2020; Volume 1003.

81. Tang, C.Z.; Tao, H.X.; Zhan, X.Q.; Xie, X.A. Mechanism of Esters Formation during Cellulose Liquefaction in Sub-and Supercritical Ethanol. *Bioresources* **2014**, *9*, 4946–4957. [\[CrossRef\]](#)
82. Vera Candiotti, L.; De Zan, M.M.; Cámara, M.S.; Goicoechea, H.C. Experimental Design and Multiple Response Optimization. Using the Desirability Function in Analytical Methods Development. *Talanta* **2014**, *124*, 123–138. [\[CrossRef\]](#) [\[PubMed\]](#)
83. Salman, N.A.S.; Mohamed Saheed, M.S.; Saqib, N.U.; Abdul Latip, A.F.; Adnan, R. Polydimethylsiloxane-Carbon Nanotubes-Based Hydrophobic Sponge for Treatment of Palm Oil Mill Rflfluents with Enhanced Reusability. *J. Environ. Chem. Eng.* **2023**, *11*, 1–15. [\[CrossRef\]](#)
84. Jaber, W.S.; Alwared, A.I. Removal of Oil Emulsion from Aqueous Solution by Using Ricinus Communis Leaves as Adsorbent. *Springer Nat. Appl. Sci.* **2019**, *1*, 1–12. [\[CrossRef\]](#)
85. Vitz, E.; Moore, J.W.; Shorb, J.; Prat-Resina, X.; Wendorff, T.; Hahn, A. 20.5: Nonpolar Lipids. Available online: [https://chem.libretexts.org/Bookshelves/General\\_Chemistry/Book:\\_ChemPRIME\\_\(Moore\\_et\\_al.\)/20:\\_Molecules\\_in\\_Living\\_Systems/20.05:\\_Nonpolar\\_Lipids](https://chem.libretexts.org/Bookshelves/General_Chemistry/Book:_ChemPRIME_(Moore_et_al.)/20:_Molecules_in_Living_Systems/20.05:_Nonpolar_Lipids) (accessed on 25 April 2023).
86. Sidik, S.M.; Jalil, A.A.; Triwahyono, S.; Adam, S.H.; Satar, M.A.H.; Hameed, B.H. Modified Oil Palm Leaves Adsorbent with Enhanced Hydrophobicity for Crude Oil Removal. *Chem. Eng. J.* **2012**, *203*, 9–18. [\[CrossRef\]](#)
87. Xiaobing, L.I.; Chunjuan, Z.; Jiongtian, L. Adsorption of Oil from Waste Water by Coal: Characteristics and Mechanism. *Min. Sci. Technol.* **2010**, *20*, 778–781. [\[CrossRef\]](#)
88. Chukwuma, O.E. Effect of Alkali Treatment on Kenaf Fibre Quality. *Sci. Arena Publ. Spec. J. Agric. Sci.* **2017**, *3*, 12–21.
89. Syed Hashim, S.N.A.; Zakaria, S.; Chia, C.H.; Pua, F.L.; Syed Jaafar, S.N. Chemical and Thermal Properties of Purified Kenaf Core and Oil Palm Empty Fruit Bunch Lignin. *Sains Malays.* **2016**, *45*, 1649–1653.
90. Wong, C.; McGowan, T.; Bajwa, S.G.; Bajwa, D.S. Impact of Fiber Treatment on the Oil Absorption Characteristics of Plant Fibers. *Bioresources* **2016**, *11*, 6452–6463. [\[CrossRef\]](#)
91. Ilyas, R.A.; Sapuan, S.M.; Ishak, M.R.; Zainudin, E.S. Effect of Delignification on the Physical, Thermal, Chemical, and Structural Properties of Sugar Palm Fibre. *Bioresources* **2017**, *12*, 8734–8754. [\[CrossRef\]](#)
92. Wahi, R.; Abdullah, L.C.; Choong, T.S.Y.; Ngaini, Z.; Nourouzi, M.M. Oil Removal from Aqueous State by Natural Fibrous Sorbent: An Overview. *Sep. Purif. Technol.* **2013**, *113*, 51–63. [\[CrossRef\]](#)
93. Abbas, A.G.N.; Abdul Aziz, F.N.A.; Abdan, K.; Mohd Nasir, N.A.; Norizan, M.N. Kenaf Fibre Reinforced Cementitious Composites. *Fibers* **2022**, *10*, 3. [\[CrossRef\]](#)
94. Koistinen, A.; Wang, H.; Hiltunen, E.; Vuorinen, T.; Maloney, T. Refinability of Mercerized Softwood Kraft Pulp. *Cellulose* **2024**, *31*, 6471–6484. [\[CrossRef\]](#)
95. Zaini, N.; Kamarudin, K.S.N. Adsorption of Carbon Dioxide on Monoethanolamine (MEA)-Impregnated Kenaf Core Fiber by Pressure Swing Adsorption System (PSA). *J. Teknol.* **2014**, *68*, 2180–3722. [\[CrossRef\]](#)
96. Mwaikambo, L.Y.; Ansell, M.P. Chemical Modification of Hemp, Sisal, Jute, and Kapok Fibers by Alkalization. *J. Appl. Polym. Sci.* **2002**, *84*, 2222–2234. [\[CrossRef\]](#)

**Disclaimer/Publisher’s Note:** The statements, opinions and data contained in all publications are solely those of the individual author(s) and contributor(s) and not of MDPI and/or the editor(s). MDPI and/or the editor(s) disclaim responsibility for any injury to people or property resulting from any ideas, methods, instructions or products referred to in the content.